

Optimal Experiment Design for Quantum State and Process Tomography and Hamiltonian Parameter Estimation *

Robert L. Kosut[†] Ian Walmsley[‡] Herschel Rabitz[§]

Abstract

A number of problems in quantum state and system identification are addressed. Specifically, it is shown that the maximum likelihood estimation (MLE) approach, already known to apply to quantum state tomography, is also applicable to quantum process tomography (estimating the Kraus operator sum representation (OSR)), Hamiltonian parameter estimation, and the related problems of state and process (OSR) distribution estimation. Except for Hamiltonian parameter estimation, the other MLE problems are formally of the same type of convex optimization problem and therefore can be solved very efficiently to within any desired accuracy.

Associated with each of these estimation problems, and the focus of the paper, is an optimal experiment design (OED) problem invoked by the Cramér-Rao Inequality: find the number of experiments to be performed in a particular system configuration to maximize estimation accuracy; a configuration being any number of combinations of sample times, hardware settings, prepared initial states, *etc.*. We show that in all of the estimation problems, including Hamiltonian parameter estimation, the optimal experiment design can be obtained by solving a convex optimization problem.¹

*Research supported by the DARPA QUIST Program.

[†]SC Solutions, Sunnyvale, CA, USA, kosut@scsolutions.com

[‡]Oxford University, Oxford, UK, walmsley@physics.ox.ac.uk

[§]Princeton University, Princeton, NJ, hrabitz@princeton.edu

¹Software to solve the MLE and OED convex optimization problems is available upon request from the first author.

Contents

1	Introduction	1
1.1	Alleviating the “havoc”	1
1.2	Convexity and quantum mechanics	2
1.3	Software for tomography & experiment design	3
2	Quantum State Tomography	3
2.1	Data collection	4
2.2	Maximum likelihood state estimation	6
2.3	Experiment design for state estimation	8
2.4	Example: experiment design for state estimation	13
2.5	Maximum likelihood state distribution estimation	21
2.6	Experiment design for state distribution estimation	22
3	Quantum Process Tomography: OSR Estimation	22
3.1	Maximum likelihood OSR estimation	22
3.2	Experiment design for OSR estimation	24
3.3	Example: experiment design for OSR estimation	25
3.4	Maximum likelihood OSR distribution estimation	27
3.5	Experiment design for OSR distribution estimation	27
3.6	Example: experiment design for OSR distribution estimation	28
4	Hamiltonian Parameter Estimation	30
4.1	Maximum likelihood Hamiltonian parameter estimation	30
4.2	Experiment design for Hamiltonian parameter estimation	31
4.3	Example: experiment design for Hamiltonian parameter estimation	31
5	Summarizing Maximum Likelihood Estimation & Optimal Experiment Design	36
6	Iterative Adaptive Control	38
6.1	Indirect adaptive control	38
6.2	Direct adaptive control	41
A	Appendix	44
A.1	Worst-case gate fidelity	44
A.2	Cramér-Rao Inequality	44
A.3	Derivation of (28)	45
A.4	Derivation of (80)	46

1 Introduction

“In a machine such as this [a quantum computer] there are very many other problems due to imperfections. For example, in the registers for holding the data, there will be problems of cross-talk, interactions between one atom and another in that register, or interaction of the atoms in that register directly with things that are happening along the program line that we didn’t exactly bargain for. In other words, there may be small terms in the Hamiltonian besides the ones we’ve written. Until we propose a complete implementation of this, it is very difficult to analyze. At least some of these problems can be remedied in the usual way by techniques such as error correcting codes and so forth, that have been studied in normal computers. But until we find a specific implementation for this computer, I do not know how to proceed to analyze these effects. However, it appears that they would be very important in practice. This computer seems to be very delicate and these imperfections may produce considerable havoc.”

– Richard P. Feynman, “Quantum Mechanical Computers,” *Optics News*, February 1985.

1.1 Alleviating the “havoc”

The concerns heralded by Feynman remain of concern today in all the implementations envisioned for quantum information systems. In a quantum computer it is highly likely that in order to achieve the desired system objectives, these systems will have to be tuned, or even entirely determined, using estimated quantities obtained from data from the actual system rather than solely relying on an initial design from a theoretical model. The problem addressed here is to design the experiment in order to yield the optimum information for the intended purpose. This goal is not just limited to quantum information systems. It is an essential step in the engineering practice of system identification [22, Ch.14]. That is, the design of the experiment which gives the best performance against a given set of criteria, subject to constraints reflecting the underlying properties of the system dynamics and/or costs associated with the implementation of certain operations or controls.

Clearly each application has a specific threshold of performance. For example, the requirements in quantum chemistry are generally not as severe as in quantum information systems. The objective of a measurement, therefore, depends on the way in which information is encoded into the system to begin with, and this is in turn, depends on the application. In this paper we are concerned with estimating quantum system properties: the state, the process which transforms the state, and parameters in a Hamiltonian model.

The estimation of the state of a quantum system from available measurements is generally referred to as *quantum state tomography* about which there is extensive literature on both theoretical and experimental aspects, *e.g.*, see [27, Ch.8], [15] and the references therein. The more encompassing procedure of *quantum system identification* is not so easily categorized as the nomenclature (and methodology) seems to depend on the type and/or intended use of the identified model. For example, *quantum process tomography* (QPT) refers to determining the Kraus *operator-sum-representation* (OSR) of the input state to output state (completely positive) map, *e.g.*, [27, §8.4.2], [7]. *Hamiltonian parameter estimation* refers to determining parameters in a model of the system Hamiltonian, *e.g.*, [24], [6], [12], [37]. Somewhere in between quantum process tomography and Hamiltonian parameter estimation is *mechanism identification* which seeks an estimate of population transfer between states as the system evolves, *e.g.*, [25].

Maximum likelihood estimation (MLE), a well established method of parameter estimation which is used extensively in current engineering applications, *e.g.*, [22], was proposed in [4, 29] and [33] for quantum state tomography of a quantum system with non-continuing measurements, *i.e.*, data is taken from repeated identical experiments. Also, as observed in [29, 33], the MLE of the density matrix is a convex optimization problem.

In this paper we address the related problem of optimal experiment design (OED) so as to secure an estimate of the best quality. The approach presented relies on minimizing the Cramer-Rao lower bound [8] where the design parameters are the number of experiments to be performed while the system is in a specified configuration. En route we also show that many related problems in state and process tomography can also be solved using MLE, and moreover, they are all *formally* the same type of convex optimization problem, namely, a determinant maximization problem, referred to as a *maxdet problem* [5, 36]. Similarly, the OED problem posed here is also of a single general type of convex optimization problem, namely, a *semidefinite program* (SDP).

Convexity arises in many ways in quantum mechanics and this is briefly discussed in §1.2. The great advantage of convex optimization is a globally optimal solution can be found efficiently and reliably, and perhaps most importantly, can be computed to within any desired accuracy. Achieving these advantages, however, requires the use of specialized numerical solvers. As described in §1.3, the appropriate convex solvers have been embedded in some software tools we have composed which can solve the MLE and OED problems presented here.

In the remainder of the paper we present both MLE and the corresponding OED as applied to: quantum state tomography (MLE in §2.2 and OED in §2.3), estimating the distribution of known input states (MLE in §2.5 and OED in §2.6), quantum process tomography using the Kraus operator sum representation (MLE in §3.1 and OED in §3.2), estimating the distribution of a known OSR set (MLE in §3.4 and OED in §3.5), and to Hamiltonian parameter estimation (MLE in §4.1 and OED in §4.2). A summary in table form is presented in §5 followed by a discussion in §6 of the relation of MLE and OED to iterative adaptive control of quantum systems.

1.2 Convexity and quantum mechanics

Many quantum operations form convex sets or functions. Consider, for example, the following convex sets which arise from some of the basic aspects of quantum mechanics:

probability outcomes	$\{p_\alpha \in \mathbf{R}\}$	$\sum_\alpha p_\alpha = 1, \quad p_\alpha \geq 0$
density matrix	$\{\rho \in \mathbf{C}^{n \times n}\}$	$\text{Tr } \rho = 1, \quad \rho \geq 0$
positive operator valued measure (POVM)	$\{O_\alpha \in \mathbf{C}^{n \times n}\}$	$\sum_\alpha O_\alpha = I_n, \quad O_\alpha \geq 0$
operator sum representation (OSR) in fixed basis	$\{X \in \mathbf{C}^{n^2 \times n^2}\}$	$\sum_{ij} X_{ij} B_i^* B_j = I_n, \quad X \geq 0$
$\{B_i \in \mathbf{C}^{n \times n} \mid i = 1, \dots, n^2\}$		

An example of a convex function relevant to quantum information is *worst-case gate fidelity*, a measure of the “distance” between two unitary operations on the same input. As pointed out in [13], there are many ways to define this measure. Consider, for example,

$$f^{\text{wc}}(U_{\text{des}}, U_{\text{act}}) = \min_{\|\psi\|=1} |(U_{\text{des}}\psi)^* (U_{\text{act}}\psi)|^2 \quad (1)$$

where $U_{\text{des}} \in \mathbf{C}^{n \times n}$ is the desired unitary and $U_{\text{act}} \in \mathbf{C}^{n \times n}$ is the actual unitary. In this case the worst-case fidelity can be interpreted as the minimum probability of obtaining the desired output state $U_{\text{des}}\psi$ over all possible pure input states ψ which produce the actual output state $U_{\text{act}}\psi$. If U_{des} and U_{act} differ by a scalar phase then the worst-case fidelity is clearly unity; which is consistent with the fact that a scalar phase cannot be measured. This is not the case for the error norm $\|U_{\text{des}} - U_{\text{act}}\|$.

As shown in Appendix §A.1, obtaining the worst-case fidelity requires solving the following (convex) *quadratic programming* (QP) problem:

$$\begin{aligned} & \text{minimize} && z^T (aa^T + bb^T) z \\ & \text{subject to} && \sum_{k=1}^n z_k = 1, \quad z_k \geq 0 \end{aligned} \quad (2)$$

with the vectors a, b in \mathbf{R}^n the real and imaginary parts, respectively, of the eigenvalues of the unitary matrix $U_{\text{des}}^* U_{\text{act}}$, that is, $a = \text{Re eig}(U_{\text{des}}^* U_{\text{act}})$, $b = \text{Im eig}(U_{\text{des}}^* U_{\text{act}})$. In some cases it is possible to compute the worst-case fidelity directly, *e.g.*, in the example in Section §4.3 and in some examples in [27, §9.3]. Although the optimal objective value $f^{\text{wc}}(U_{\text{des}}, U_{\text{act}})$ is global, the optimal worst-case state which achieves this value is not unique.

In addition to these examples, convex optimization has been exploited in [3] and [33] in an attempt to realize quantum devices with certain properties. In [9] and [21], convex optimization is used to design optimal state detectors which have the maximum efficiency.

In general, convex optimization problems enjoy many useful properties. From the introduction in [5], and as already stated, the solution to a convex optimization problem can be obtained to within any desired accuracy. In addition, computation time does not explode with problem size, stopping criteria always produce a lower bound on the solution, and if no solution can be found a proof of infeasibility is provided. There is also a complete duality theory which can yield more efficient computation as well as optimality conditions. This is explored briefly in Section §2.3.

1.3 Software for tomography & experiment design

We have composed some MATLAB m-files which can be used to solve a subset of the QPT and OED convex optimization problems presented here. The examples shown here were generated using this software. The software, available upon request from the first author, requires the convex solvers YALMIP [23] and SDPT3 [35] which can be downloaded from the internet. These solvers make use of *interior-point methods* for solving convex optimization problems, *e.g.*, [5, Ch.11], [26].

2 Quantum State Tomography

Consider a quantum system which has n_{out} distinct *outcomes*, labeled by the index α , $\alpha = 1, \dots, n_{\text{out}}$, and which can be externally manipulated into n_{cfg} distinct *configurations*, labeled

by the index γ , $\gamma = 1, \dots, n_{\text{cfg}}$. Configurations can include wave-plate angles for photon counting, sample times at which measurements are made, and settings of any experimental “knobs” such as external control variables, *e.g.*, laser wave shape parameters, magnetic field strengths, and so on. For quantum process tomography (§3.1) and Hamiltonian parameter estimation (§4.1), configurations can also include distinctly prepared initial states.

The problem addressed in this section is to determine the minimum number of experiments per configuration in order to obtain a state estimate of a specified quality, *i.e.*, what is the tradeoff between number of experiments per configuration and estimation quality. The method used to solve this problem is based on minimizing the size of the Cramér-Rao lower bound on the estimation error [8].

2.1 Data collection

The data is collected using a procedure referred to here as *non-continuing measurements*. Measurements are recorded from identical experiments in each configuration γ repeated ℓ_γ times. The set-up for data collection is shown schematically in Figure 1 for configuration γ .

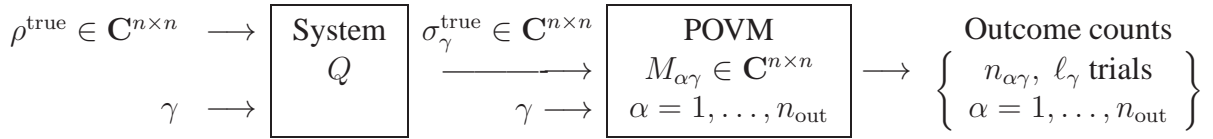


Figure 1: System/POVM.

Here $\rho^{\text{true}} \in \mathbb{C}^{n \times n}$ is the true, unknown state to be estimated, $\sigma_\gamma^{\text{true}} \in \mathbb{C}^{n \times n}$ is the *reduced density matrix* which captures all the statistical behavior of the Q -system under the action of the measurement apparatus, and $n_{\alpha\gamma}$ is the number of times outcome α is obtained from the ℓ_γ experiments. Thus,

$$\sum_{\alpha} n_{\alpha\gamma} = \ell_\gamma, \quad \ell_{\text{expt}} = \sum_{\gamma} \ell_\gamma \quad (3)$$

where ℓ_{expt} is the total number of experiments. The *data set* consists of all the outcome counts,

$$D = \{ n_{\alpha\gamma} \mid \alpha = 1, \dots, n_{\text{out}}, \gamma = 1, \dots, n_{\text{cfg}} \} \quad (4)$$

The design variables used to optimize the experiment are the non-negative integers $\{\ell_\gamma\}$ represented by the vector,

$$\ell = [\ell_1 \dots \ell_{n_{\text{cfg}}}]^T \quad (5)$$

Let $p_{\alpha\gamma}^{\text{true}}$ denote the true probability of obtaining outcome α when the system is in configuration γ with state input ρ^{true} . Thus,

$$\mathbf{E} n_{\alpha\gamma} = \ell_\gamma p_{\alpha\gamma}^{\text{true}} \quad (6)$$

where the expectation $\mathbf{E}(\cdot)$ taken with respect to the underlying quantum probability distributions.

We pose the following *model* of the system,

$$p_{\alpha\gamma}(\rho) = \text{Tr } M_{\alpha\gamma} \sigma_\gamma(\rho) \quad (7)$$

where $p_{\alpha\gamma}(\rho)$ is the outcome probability of measuring α when the system is in configuration γ with input state ρ belonging to the set of density matrices,

$$\left\{ \rho \in \mathbf{C}^{n \times n} \mid \rho \geq 0, \text{Tr } \rho = 1 \right\} \quad (8)$$

$\{M_{\alpha\gamma}\}$ are the POVM elements of the measurement apparatus, and thus, for $\gamma = 1, \dots, n_{\text{cfg}}$,

$$\sum_{\alpha} M_{\alpha\gamma} = I_n, \quad M_{\alpha\gamma} \geq 0, \quad \alpha = 1, \dots, n_{\text{out}} \quad (9)$$

and $\sigma_{\gamma}(\rho)$ is the reduced density output state of the Q -system model. A general (model) representation of the Q system is the *Kraus operator-sum-representation* (OSR) which can account for many forms of error sources as well as decoherence [27]. Specifically, in configuration γ , the Q -system model can be parametrized by the set of *Kraus matrices*, $K_{\gamma} = \{K_{\gamma k} \in \mathbf{C}^{n \times n} \mid k = 1, \dots, \kappa_{\gamma}\}$ as follows:

$$\sigma_{\gamma}(\rho) = Q(\rho, K_{\gamma}) = \sum_{k=1}^{\kappa_{\gamma}} K_{\gamma k} \rho K_{\gamma k}^*, \quad \sum_{k=1}^{\kappa_{\gamma}} K_{\gamma k}^* K_{\gamma k} = I_n \quad (10)$$

with $\kappa_{\gamma} \leq n^2$. Implicit in this OSR is the assumption that the Q -system is trace preserving. Combining this with the measurement model (9) gives the model probability outcomes,

$$p_{\alpha\gamma}(\rho) = \text{Tr } O_{\alpha\gamma} \rho, \quad O_{\alpha\gamma} = \sum_{k=1}^{\kappa_{\gamma}} K_{\gamma k}^* M_{\alpha\gamma} K_{\gamma k} \quad (11)$$

In this model, the outcome probabilities are *linear* in the input state density matrix. Moreover, the set $O_{\gamma} = \{O_{\alpha\gamma} \mid \alpha = 1, \dots, n_{\text{out}}\}$, satisfies (9), and hence, is a POVM.² If the Q -system is modeled as a unitary system, then,

$$\sigma_{\gamma}(\rho) = U_{\gamma} \rho U_{\gamma}^*, \quad U_{\gamma}^* U_{\gamma} = I_n \implies O_{\alpha\gamma} = U_{\gamma}^* M_{\alpha\gamma} U_{\gamma} \quad (12)$$

The set O_{γ} is still a POVM; in effect the OSR has a single element, namely, $K_{\gamma} = U_{\gamma}$.

System in the model set

We make the following assumption throughout: *the true system is in the model set*. This means that,

$$p_{\alpha\gamma}^{\text{true}} = p_{\alpha\gamma}(\rho^{\text{true}}) = \text{Tr } O_{\alpha\gamma} \rho^{\text{true}} \quad (13)$$

This is always a questionable assumption and in most engineering practice is never true. Relaxing this assumption is an active research topic particularly when identification (state or process) is to be used for control design, *e.g.*, see [19] and [34]. The case when the system is *not* in the model set will not be explored any further here except for the effect of measurement noise which is discussed next. It is important to emphasize that in order to produce an accurate unbiased estimate of the true density it is necessary to know the noise elements (as described next) which is a consequence of assumption (13).

²In a more general OSR the Q -system need not be trace preserving, hence the Kraus matrices in (10) need not sum to identity as shown, but rather, their sum is bounded by identity. Then the set O_{γ} is not a POVM, however, satisfies, $\sum_{\alpha} O_{\alpha\gamma} \leq I_n$, $O_{\alpha\gamma} \geq 0$, $\alpha = 1, \dots, n_{\text{out}}$

Noisy measurements

Sensor noise can engender more noisy outcomes than noise-free outcomes. Consider, for example, a photon detection device with two photon-counting detectors. If both are noise-free, meaning, perfect efficiency and no dark count probability, then, provided one photon is always present at the input of the device, there are only two possible outcomes: $\{10, 01\}$. If, however, each detector is noisy, then either or both detectors can misfire or fire even with a photon always present at the input. Thus in the noisy case there are *four* possible outcomes: $\{10, 01, 11, 00\}$.

Let $\{M_{\alpha\gamma} \mid \alpha = 1, \dots, n_{\text{out}}\}$ denote the noisy POVM and let $\{\overline{M}_{\alpha\gamma} \mid \alpha = 1, \dots, \overline{n}_{\text{out}}\}$ denote the noise-free POVM with $n_{\text{out}} \geq \overline{n}_{\text{out}}$ where,

$$M_{\alpha\gamma} = \sum_{\beta=1}^{\overline{n}_{\text{out}}} \nu_{\alpha\beta\gamma} \overline{M}_{\beta\gamma}, \quad \alpha = 1, \dots, n_{\text{out}}, \quad \gamma = 1, \dots, n_{\text{cfg}} \quad (14)$$

The $\{\nu_{\alpha\beta\gamma}\}$ represents the noise in the measurement, specifically, the conditional probability that α is measured given the noise-free outcome β with the system in configuration γ . Since $\sum_{\alpha} \nu_{\alpha\beta\gamma} = 1, \forall \beta, \gamma$, it follows that if the noise-free set is a POVM then so is the noisy set.

2.2 Maximum likelihood state estimation

The Maximum Likelihood (ML) approach to quantum state estimation presented in this section, as well as observing that the estimation is convex, can be found in [29], [37] and the references therein. Using convex programming methods, such as an interior-point algorithm for computation, was not exploited in these references.

If the experiments are independent, then the probability of obtaining the data (4) is a product of the individual model probabilities (7). Consequently, for an *assumed* initial state ρ , the model predicts that the probability of obtaining the data set (4) is given by,

$$\text{Prob}\{D, \rho\} = \prod_{\alpha, \gamma} p_{\alpha\gamma}(\rho)^{n_{\alpha\gamma}} \quad (15)$$

The data is thus captured in the outcome counts $\{n_{\alpha\gamma}\}$ whereas the model terms have a ρ -dependence. The function $\text{Prob}\{D, \rho\}$ is called the *likelihood* function and since it is positive, the *maximum likelihood estimate* (MLE) of ρ is obtained by finding a ρ in the set (8) which maximizes the *log-likelihood function*, or equivalently, minimizes the *negative log-likelihood function*,

$$\begin{aligned} L(D, \rho) &= -\log \text{Prob}\{D, \rho\} \\ &= -\sum_{\alpha, \gamma} n_{\alpha\gamma} \log p_{\alpha\gamma}(\rho) \\ &= -\sum_{\alpha, \gamma} n_{\alpha\gamma} \log \text{Tr } O_{\alpha\gamma} \rho \end{aligned} \quad (16)$$

These expressions are obtained by combining (15), (16) and (11). The Maximum Likelihood state estimate, ρ^{ML} , is obtained as the solution to the optimization problem:

$$\begin{aligned} &\text{minimize} \quad L(D, \rho) = -\sum_{\alpha, \gamma} n_{\alpha\gamma} \log \text{Tr } O_{\alpha\gamma} \rho \\ &\text{subject to} \quad \rho \geq 0, \text{Tr } \rho = 1 \end{aligned} \quad (17)$$

$L(D, \rho)$ is a positively weighted sum of log-convex functions of ρ , and hence, is a log-convex function of ρ . The constraint that ρ is a density matrix forms a convex set in ρ . Hence, (17) is in a category of a class of well studied log-convex optimization problems, *e.g.*, [5].

Pure state estimation

Suppose it is known the the true state is pure, that is, $\rho^{\text{true}} = \psi_{\text{true}}\psi_{\text{true}}^*$ with $\psi_{\text{true}} \in \mathbb{C}^n$ and $\psi_{\text{true}}^*\psi_{\text{true}} = 1$. In practice we have found that solving (17) when the true state is pure gives solutions which are easily approximated by pure states, that is, the estimated state has one singular value near one and all the rest are very small and positive.

To deal directly with pure state estimation we first need to characterize the set of all density matrices which are pure. This is given by the set $\{\rho \in \mathbb{C}^{n \times n} \mid \rho \geq 0, \text{rank } \rho = 1\}$, which is equivalent to,

$$\left\{ \rho \in \mathbb{C}^{n \times n} \mid \rho \geq 0, \text{Tr } \rho = 1, \text{Tr } \rho^2 = 1 \right\} \quad (18)$$

The corresponding ML estimate is then the solution of,

$$\begin{aligned} &\text{minimize } L(\rho) = -\sum_{\alpha,\gamma} n_{\alpha\gamma} \log \text{Tr } O_{\alpha\gamma} \rho \\ &\text{subject to } \rho \geq 0, \text{Tr } \rho = 1, \text{Tr } \rho^2 = 1 \end{aligned} \quad (19)$$

This is not a convex optimization problem because the equality constraint, $\text{Tr } \rho^2 = 1$, is not convex. However, relaxing this constraint to the convex *inequality* constraint, $\text{Tr } \rho^2 \leq 1$, results in the convex optimization problem:

$$\begin{aligned} &\text{minimize } L(\rho) = -\sum_{\alpha,\gamma} n_{\alpha\gamma} \log \text{Tr } O_{\alpha\gamma} \rho \\ &\text{subject to } \rho \geq 0, \text{Tr } \rho = 1, \text{Tr } \rho^2 \leq 1 \end{aligned} \quad (20)$$

If the solution is on the boundary of the set $\text{Tr } \rho^2 \leq 1$, then a pure state has been found. There is however, no guaranty that this will occur.

Least-squares (LS) state estimation

In a typical application the number of trials per configuration, ℓ_γ , is sufficiently large so that the *empirical estimate* of the outcome probability,

$$p_{\alpha\gamma}^{\text{emp}} = \frac{n_{\alpha\gamma}}{\ell_\gamma} \quad (21)$$

is a good estimate of the true outcome probability $p_{\alpha\gamma}^{\text{true}}$. The empirical probability estimate also provides the smallest possible value of the negative log-likelihood function, that is, $p_{\alpha\gamma}^{\text{emp}}$ is the solution to,

$$\begin{aligned} &\text{minimize } L(p) = -\sum_{\alpha,\gamma} n_{\alpha\gamma} \log p_{\alpha\gamma} \\ &\text{subject to } \sum_{\alpha} p_{\alpha\gamma} = 1, \forall \gamma, p_{\alpha\gamma} \geq 0, \forall \alpha, \gamma \end{aligned} \quad (22)$$

with optimization variables $p_{\alpha\gamma}, \forall \alpha, \gamma$. Thus, for any value of ρ we have the lower bound,

$$-\sum_{\alpha,\gamma} n_{\alpha\gamma} \log \frac{n_{\alpha\gamma}}{\ell_\gamma} \leq -\sum_{\alpha,\gamma} n_{\alpha\gamma} \log \text{Tr } O_{\alpha\gamma} \rho \quad (23)$$

In particular, assuming (6) holds, and the ℓ_γ trials are independent, then the variance of the empirical estimate is known to be [28],

$$\text{var } p_{\alpha\gamma}^{\text{emp}} = \frac{1}{\ell_\gamma} p_{\alpha\gamma}^{\text{true}} (1 - p_{\alpha\gamma}^{\text{true}}) \quad (24)$$

It therefore follows that for large ℓ_γ , $p_{\alpha\gamma}^{\text{emp}} \approx p_{\alpha\gamma}^{\text{true}}$, and if as assumed (13), the system is in the model set, then $p_{\alpha\gamma}^{\text{true}} = \text{Tr } O_{\alpha\gamma} \rho^{\text{true}}$. These two conditions lead to taking the state estimate as the solution to the constrained weighted least-squares problem:

$$\begin{aligned} & \text{minimize} && \sum_{\alpha,\gamma} w_\gamma \left(p_{\alpha\gamma}^{\text{emp}} - \text{Tr } O_{\alpha\gamma} \rho \right)^2 \\ & \text{subject to} && \rho \geq 0, \text{Tr } \rho = 1 \end{aligned} \quad (25)$$

The weights, w_γ , are chosen by the user to emphasize different configurations. A typical choice is the distribution of experiments per configuration, hence, $w_\gamma \geq 0$, $\sum_\gamma w_\gamma = 1$. Because of the semi-definite constraint, this weighted-least-squares problem is a convex optimization in the variable ρ . For large ℓ_γ , the solution ought to be a good estimate of the true state. There is, however, little numerical benefit in solving (25) as compared to (17) – they are both convex optimization problems and the numerical complexity is similar provided (17) is solved using an interior-point method [5]. Some advantage is obtained by dropping the semidefinite constraint $\rho \geq 0$ in (25) resulting in,

$$\begin{aligned} & \text{minimize} && \sum_{\alpha,\gamma} w_\gamma \left(p_{\alpha\gamma}^{\text{emp}} - \text{Tr } O_{\alpha\gamma} \rho \right)^2 \\ & \text{subject to} && \text{Tr } \rho = 1 \end{aligned} \quad (26)$$

This is a standard least-squares problem with a linear equality constraint which can be solved very efficiently using a singular value decomposition to eliminate the equality constraint [14]. For sufficiently large ℓ_γ the resulting estimate *may* satisfy the positivity constraint $\rho \geq 0$. If not, it is usually the case that some of the small eigenvalues of the state estimate or estimated outcome probabilities are slightly negative which can be manually set to zero. Solving (26) is numerically faster than solving (17), but not by much. Even with a large amount of data the solution to (26) can produce estimates which are not positive if the data is not sufficiently rich. In this case the estimates from any procedure which eliminates the positivity constraint can be very misleading.

It thus appears that even for large ℓ_γ , there is no significant benefit accrued, either because of numerical precision or speed, to using the empirical estimate followed by standard least-squares. If, however, the ℓ_γ are not sufficiently large and/or the data is not sufficiently rich, then it is unlikely that the estimate from (26) will be accurate.

One possible advantage does come about because the solution to (26) can be expressed analytically, and thus it is possible to gain an understanding of how to select the POVM. For example, in [27] special POVM elements are selected to essentially diagonalize the problem, thereby making the least-squares problem (26) simpler, *i.e.*, the elements of the density matrix can be estimated one at a time. However, implementing the requisite POVM set may be very difficult depending on the physical apparatus involved.

2.3 Experiment design for state estimation

In this section we describe the experiment design problem for quantum state estimation. The objective is to select the number of experiments per configuration, the elements of the vector $\ell = [\ell_1 \cdots \ell_{n_{\text{cfg}}}]^T \in \mathbf{R}^{n_{\text{cfg}}}$, so as to minimize the error between the state estimate, $\hat{\rho}(\ell)$, and the

true state ρ^{true} . Specifically, we would like to solve for ℓ from:

$$\begin{aligned} & \text{minimize} && \mathbf{E} \|\hat{\rho}(\ell) - \rho^{\text{true}}\|_{\text{frob}}^2 \\ & \text{subject to} && \sum_{\gamma} \ell_{\gamma} = \ell_{\text{expt}} \\ & && \text{integer } \ell_{\gamma} \geq 0, \gamma = 1, \dots, n_{\text{cfg}} \end{aligned} \quad (27)$$

where ℓ_{expt} is the desired number of total experiments. This is a difficult, if not insoluble problem for several reasons. First, the solution depends on the estimation method which produces $\hat{\rho}(\ell)$. Secondly, the problem is integer combinatorial because ℓ is a vector of integers. And finally, the solution depends on ρ^{true} , the very state to be estimated. Fortunately all these issues can be circumvented.

We first eliminate the dependence on the estimation method. The following result can be established using the *Cramér-Rao Inequality* [8]. The derivation is in Appendix §A.3.

State estimation variance lower bound ³

Suppose the system generating the data is in the model set used for estimation, *i.e.*, (13) holds. For $\ell = [\ell_1 \dots \ell_{n_{\text{cfg}}}]$ experiments per configuration, suppose $\hat{\rho}(\ell)$ is a density matrix *and* an unbiased estimate of ρ^{true} , *i.e.*, $\hat{\rho}(\ell) \geq 0$, $\text{Tr } \hat{\rho}(\ell) = 1$, and $\mathbf{E} \hat{\rho}(\ell) = \rho^{\text{true}}$. Under these conditions, the estimation error variance satisfies,

$$\mathbf{E} \|\hat{\rho}(\ell) - \rho^{\text{true}}\|_{\text{frob}}^2 \geq V(\ell, \rho^{\text{true}}) = \text{Tr } G(\ell, \rho^{\text{true}})^{-1} \quad (28)$$

where⁴

$$\begin{aligned} G(\ell, \rho^{\text{true}}) &= \sum_{\gamma=1}^{n_{\text{cfg}}} \ell_{\gamma} G_{\gamma}(\rho^{\text{true}}) \in \mathbf{R}^{n^2-1 \times n^2-1} \\ G_{\gamma}(\rho^{\text{true}}) &= C_{\text{eq}}^T \left(\sum_{\alpha} \frac{a_{\alpha\gamma} a_{\alpha\gamma}^*}{p_{\alpha\gamma}(\rho^{\text{true}})} \right) C_{\text{eq}} \in \mathbf{R}^{n^2 \times n^2} \end{aligned} \quad (29)$$

$$a_{\alpha\gamma} = \text{vec } O_{\alpha\gamma} \in \mathbf{C}^{n^2}$$

and $C_{\text{eq}} \in \mathbf{R}^{n^2 \times n^2-1}$ is part of the unitary matrix in the singular value decomposition: $\text{vec } I_n = U S W^T \in \mathbf{R}^{n^2}$, $W = [C_{\text{eq}}] \in \mathbf{R}^{n^2 \times n^2}$.

This theorem states that for any unbiased estimate of ρ^{true} , the variance of the estimate satisfies the inequality (28). The power of the result is that it is independent of *how* the estimate is obtained, *i.e.*, no estimation algorithm which produces an unbiased estimate can have an estimation error variance smaller than that in (28). There is a generalization for biased estimators but we will not pursue that here.

In general it is difficult to determine if any estimate will achieve the lower bound. However, under the conditions stated in the above result, the ML estimate, $\rho^{\text{ML}}(\ell)$, the solution to (17), approaches ρ^{true} with probability one, asymptotically as ℓ_{expt} increases, and the asymptotic

³Cramér-Rao bounds previously reported in the literature are not quite correct as they do not include the linear constraint $\text{Tr } \rho = 1$ as is done here.

⁴The vec operation takes the rows of a matrix and stacks them one row at a time on top of each other. Two useful expressions are $\text{vec}(AXB) = (B^T \otimes A)\text{vec } X$ and $\text{Tr } AX = (\text{vec } A^T)^T \text{vec } X$.

distribution becomes Gaussian with covariance given by the Cramér-Rao bound (see §A.2 for the covariance expression and [22] for a derivation).

The one qualifier to the Cramér-Rao bound as presented is that the indicated inverse exists. This condition, however, is necessary and sufficient to insure that the state is identifiable. More precisely, the state is *identifiable* if and only if,

$$G(\ell = 1_{n_{\text{cfg}}}, \rho^{\text{true}}) = C_{\text{eq}}^* \left(\sum_{\gamma} \sum_{\alpha} \frac{a_{\alpha\gamma} a_{\alpha\gamma}^*}{p_{\alpha\gamma}(\rho^{\text{true}})} \right) C_{\text{eq}} \quad \text{is invertible} \quad (30)$$

Under the condition of identifiability, the experiment design problem can be expressed by the following optimization problem in the vector of integers ℓ :

$$\begin{aligned} & \text{minimize} && V(\ell, \rho^{\text{true}}) = \text{Tr } G(\ell, \rho^{\text{true}})^{-1} \\ & \text{subject to} && \sum_{\gamma} \ell_{\gamma} = \ell_{\text{expt}} \\ & && \text{integer } \ell_{\gamma} \geq 0, \gamma = 1, \dots, n_{\text{cfg}} \end{aligned} \quad (31)$$

where ℓ_{expt} is the desired number of total experiments. The good news is that the objective, $V(\ell, \rho^{\text{true}})$, is convex in ℓ [5, §7.5]. Unfortunately, there are still two impediments: (i) restricting ℓ to a vector of integers makes the problem combinatorial; (ii) the lower-bound function $V(\ell, \rho^{\text{true}})$ depends on the true value, ρ^{true} . These difficulties can be alleviated to some extent. For (i) we can use the convex relaxation described in [5, §7.5]. For (ii) we can solve the relaxed experiment design problem with either a set of “what-if” estimates as surrogates for ρ^{true} , or use nominal values to start and then “bootstrap” to more precise values by iterating between state estimation and experiment design. We now explain how to perform these steps.

Relaxed experiment design for state estimation

Following the procedure in [5, §7.5], introduce the variables $\lambda_{\gamma} = \ell_{\gamma}/\ell_{\text{expt}}$, each of which is the fraction of the total number of experiments performed in configuration γ . Since all the ℓ_{γ} and ℓ_{expt} are non-negative integers, each λ_{γ} is non-negative and *rational*, specifically an integer multiple of $1/\ell_{\text{expt}}$, and in addition, $\sum_{\gamma} \lambda_{\gamma} = 1$. Let ρ^{surr} denote a surrogate for ρ^{true} , *e.g.*, an estimate or candidate value of ρ^{true} . Using (28)-(29) gives,

$$V(\ell = \ell_{\text{expt}} \lambda, \rho^{\text{surr}}) = \frac{1}{\ell_{\text{expt}}} V(\lambda, \rho^{\text{surr}}) \quad (32)$$

Using (29),

$$\begin{aligned} V(\lambda, \rho^{\text{surr}}) &= \text{Tr } G(\lambda, \rho^{\text{surr}})^{-1} \\ G(\lambda, \rho^{\text{surr}}) &= \sum_{\gamma} \lambda_{\gamma} G_{\gamma}(\rho^{\text{surr}}) \end{aligned} \quad (33)$$

Hence, the objective function $V(\ell, \rho^{\text{surr}})$ can be replaced with $V(\lambda, \rho^{\text{surr}})$ and the experiment design problem (31) is equivalent to.

$$\begin{aligned} & \text{minimize} && V(\lambda, \rho^{\text{surr}}) = \text{Tr } G(\lambda, \rho^{\text{surr}})^{-1} \\ & \text{subject to} && \sum_{\gamma} \lambda_{\gamma} = 1 \\ & && \lambda_{\gamma} \geq 0, \text{ integer multiple of } 1/\ell_{\text{expt}}, \gamma = 1, \dots, n_{\text{cfg}} \end{aligned} \quad (34)$$

The objective is now a convex function of the λ_γ , but it is still a combinatorial problem because the λ_γ are constrained to each be an integer multiple of $1/\ell_{\text{expt}}$. If λ_γ is only otherwise constrained to the non-negative reals, then this has the effect of relaxing the constraint that the ℓ_γ are integers. As phrased in [5], the *relaxed* experiment design problem is:

$$\begin{aligned} & \text{minimize} && V(\lambda, \rho^{\text{surr}}) = \text{Tr} \left(\sum_\gamma \lambda_\gamma G_\gamma(\rho^{\text{surr}}) \right)^{-1} \\ & \text{subject to} && \sum_\gamma \lambda_\gamma = 1 \\ & && \lambda_\gamma \geq 0, \gamma = 1, \dots, n_{\text{cfg}} \end{aligned} \quad (35)$$

The objective is convex, the equality constraint is linear, and the inequality constraints are convex, hence, this is a convex optimization problem in $\lambda \in \mathbf{R}^{n_{\text{cfg}}}$. Let λ^{opt} denote the optimal solution to (35). Since the problem no longer depends on ℓ_{expt} , λ^{opt} can be viewed as a distribution of experiments per configuration.⁵ Clearly there is no guaranty that $\ell_{\text{expt}} \lambda^{\text{opt}}$ is a vector of integer multiples of $1/\ell_{\text{expt}}$. A practical choice for obtaining a vector of integer multiples of $1/\ell_{\text{expt}}$ is,

$$\ell_{\text{expt}}^{\text{round}} = \mathbf{round} \left\{ \ell_{\text{expt}} \lambda^{\text{opt}} \right\} \quad (36)$$

If ℓ^{opt} is the (unknown) integer vector solution to (31), then we have the relations:

$$V(\ell_{\text{expt}}^{\text{round}}, \rho^{\text{surr}}) \geq V(\ell^{\text{opt}}, \rho^{\text{surr}}) \geq V(\ell_{\text{expt}} \lambda^{\text{opt}}, \rho^{\text{surr}}) \quad (37)$$

The optimal objective is thus bounded above and below by known values obtained from the relaxed optimization. The gap within which falls the optimal solution can be no worse than the difference between $V(\ell_{\text{expt}}^{\text{round}}, \rho^{\text{surr}})$ and $V(\ell_{\text{expt}} \lambda^{\text{opt}}, \rho^{\text{surr}})$, which can be computed solely from λ^{opt} . If the gap is sufficiently small then for all practical purposes the “optimal” solution is λ^{opt} . From now on we will refer to λ^{opt} as the optimal solution rather than the relaxed optimal.

Performance tradeoff

The optimal distribution λ^{opt} can be used to guide the elimination of small values of λ^{opt} . For example, consider the *suboptimal* distribution, λ^{sub} , obtained by selecting the largest n_{sub} out of n_{cfg} non-zero values of λ^{opt} . Let $\ell_{\text{expt}}^{\text{sub}}$ denote the integer vector of configurations,

$$\ell_{\text{expt}}^{\text{sub}} = \mathbf{round} \left\{ \ell_{\text{expt}} \lambda^{\text{sub}} \right\} \quad (38)$$

Using (32), the minimum number of experiments so that $V(\ell_{\text{expt}}^{\text{sub}}, \rho^{\text{surr}}) \leq V_0$ is given by,

$$\ell_{\text{expt}}^{\text{sub}} = \mathbf{round} \left\{ V(\lambda^{\text{sub}}, \rho^{\text{surr}}) / V_0 \right\} \quad (39)$$

As n_{sub} is varied, the graph $\{n_{\text{sub}}, \ell_{\text{expt}}^{\text{sub}}\}$ establishes a tradeoff between the number of configurations per experiment versus the total number of experiments such that the lower bound on the estimation variance does not exceed the desired value V_0 . When $n_{\text{sub}} = n_{\text{cfg}}$, (39) is identical with (36).

⁵**Caveat emptor:** The relaxed optimal experiment design distribution, λ^{opt} , is optimal with respect to the initial state ρ^{surr} , a surrogate for ρ^{true} . Thus, λ^{opt} is *not* optimal with respect to ρ^{true} . This should be no surprise because the underlying goal is to find a good estimate of ρ^{true} .

The condition number of the matrix $G(\lambda^{\text{opt}}, \rho^{\text{surr}})$ gives an indication of the identifiability of the density matrix ρ^{surr} . A very large condition number means that the linear combination of elements of the density matrix associated with the small eigenvalue will be more difficult to obtain than those combinations associated with a large eigenvalue. The condition number of $G(\lambda^{\text{opt}}, \rho^{\text{surr}})$ is not only affected by the number of experiments per configuration, λ^{opt} , but by the configurations themselves. Examining $G(\lambda^{\text{opt}}, \rho^{\text{surr}})$ for different ρ^{surr} (surrogates of ρ^{true}) and different configurations can help establish a good experiment design.

Bootstrapping

A standard approach used to circumvent not knowing the true state needed to optimize the experiment design is to proceed adaptively, or by “bootstrapping.” The idea is to use the current estimate of the initial state found from (17), then solve (35), and then repeat. The algorithm at the k -th iteration looks like this:

$$\begin{aligned}\hat{\rho}(k) &= \arg \min_{\rho} V(\hat{\ell}(k-1), \rho) \\ \lambda^{\text{opt}}(k) &= \arg \min_{\lambda} V(\lambda, \rho = \hat{\rho}(k)) \\ \hat{\ell}(k) &= \mathbf{round} \{ \ell_{\text{expt}} \lambda^{\text{opt}}(k) \}\end{aligned}\tag{40}$$

The initial distribution $\hat{\ell}(0)$ could be chosen as uniform, *e.g.*, the same for a not too large number of configurations. The algorithm could also start by first solving for a distribution from an initial state surrogate. In each iteration we could also vary ℓ_{expt} . Although each optimization is convex, the joint problem may not be. Conditions for convergence would need to be investigated as well as establishing that this method is efficient, *i.e.*, reduces the number of trials. We will not pursue this any further here.

Dual experiment design problem

Lagrange Duality Theory can provide a lower bound on the objective function in an optimization problem as well as establishing optimality conditions often leading to insights into the optimal solution structure [5, Ch.5]. In many cases the largest lower bound – the solution of the *dual problem* – is equal to the optimal objective function. The dual problem associated with the experiment design problem (35) is,

$$\begin{aligned}\text{maximize} \quad & (\text{Tr } W^{1/2})^2 \\ \text{subject to} \quad & \text{Tr } W G_{\gamma}(\rho^{\text{surr}}) \leq 1, \quad \gamma = 1, \dots, n_{\text{cfg}} \\ & W > 0\end{aligned}\tag{41}$$

The optimization variable is $W \in \mathbf{C}^{n^2-1 \times n^2-1}$. The above form of the dual is given in [5, §7.5.2] for a slightly simpler problem (the G_{γ} are dyads) but is essentially the same. A key observation arises from the *complementary slackness condition*,

$$\lambda_{\gamma}^{\text{opt}} (\text{Tr } W^{\text{opt}} G_{\gamma}(\rho^{\text{surr}}) - 1) = 0, \quad \gamma = 1, \dots, n_{\text{cfg}}\tag{42}$$

where λ^{opt} is the solution to the *primal problem*, (35), and W^{opt} is the solution to the dual problem, (41). Thus, only when the equality constraint holds, $\text{Tr } W^{\text{opt}} G_\gamma(\rho^{\text{surr}}) = 1$, is the associated $\lambda_\gamma^{\text{opt}}$ not necessarily equal to zero. It will therefore be usually the case that many of the elements of the optimal distribution will be zero.

Strong duality also holds for this problem, thus the optimal primal and dual objective values are equal,

$$\text{Tr} \left(\sum_\gamma \lambda_\gamma^{\text{opt}} G_\gamma(\rho^{\text{surr}}) \right)^{-1} = \left(\text{Tr} (W^{\text{opt}})^{1/2} \right)^2 \quad (43)$$

For this problem, a pair (λ, W) is optimal with respect to ρ^{surr} if and only if:

$$\begin{aligned} \sum_\gamma \lambda_\gamma &= 1 \\ \lambda_\gamma &\geq 0, \forall \gamma \\ \lambda_\gamma^{\text{opt}} (\text{Tr } W^{\text{opt}} G_\gamma(\rho^{\text{surr}}) - 1) &= 0, \forall \gamma \\ \text{Tr } W G_\gamma(\rho^{\text{surr}}) &\leq 1, \forall \gamma \\ \text{Tr} \left(\sum_\gamma \lambda_\gamma G_\gamma(\rho^{\text{surr}}) \right)^{-1} &= \left(\text{Tr} (W^{\text{opt}})^{1/2} \right)^2 \end{aligned} \quad (44)$$

2.4 Example: experiment design for state estimation

A schematic of an apparatus for state tomography of a pair of entangled photons specified by the quantum state (density matrix) ρ is shown in figure 2.

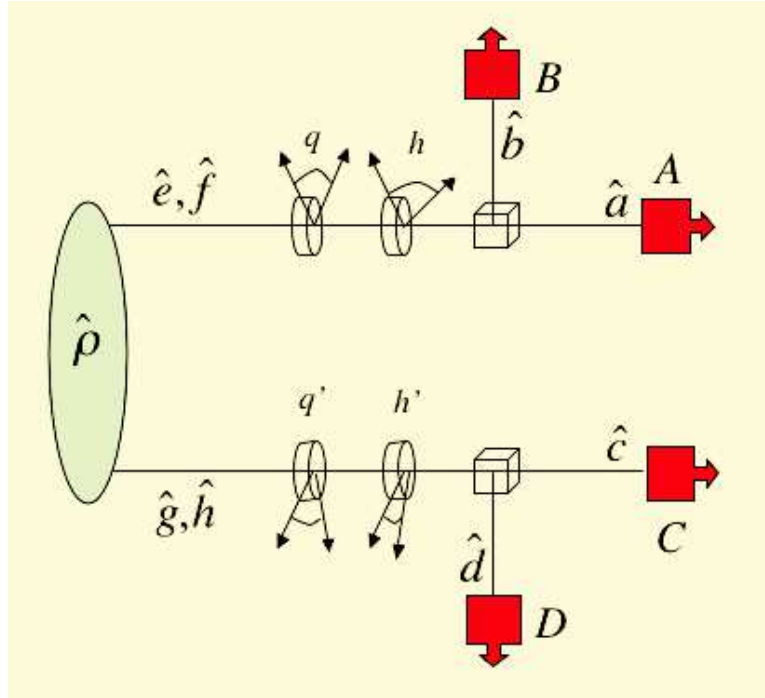


Figure 2: Detection apparatus for two-photon tomography

The set up has four photon-counting detectors, A, B, C, D. There are four continuous variable settings for the quarter-wave plates and half-wave plates, *i.e.*, q, h, q', h' . For any settings of these parameters one of the detectors in each arm will register a photon. The objective is to

determine the optimal settings of these parameters and the number of experiments per setting for estimation of the state ρ of the pair using as data the photon counts from the four detectors.

Because the photon sources are not completely efficient, the input quantum state actually consists of either two or zero photons. The detectors register a 0 or 1 depending on whether a photon is incident on them or not. The basis states for the upper arm are therefore: $|0\rangle_e|0\rangle_f$, $|0\rangle_e|1\rangle_f$, $|1\rangle_e|0\rangle_f$. There is a similar set for the lower arm (modes g, h).

The firing patterns for an arbitrary setting of the wave plates, assuming perfect detection efficiency and no dark counts are given in the table:

A	B	C	D
0	1	0	1
0	1	1	0
1	0	0	1
1	0	1	0
0	0	0	0

The probabilities for these patterns are given by

$$p_{ijkl} = \text{Tr} (M_{AB}^{ij} \otimes M_{CD}^{kl}) \rho \quad (45)$$

where $\{i, j, k, \ell\} \in \{0, 1\}$, and M_{AB}^{ij} is the projector for detector A to register count i and simultaneously detector B to register count j . Similarly, M_{CD}^{kl} is the projector for detector C to register count k and simultaneously detector D to register count ℓ . The projectors for A and B in the above basis are:

$$\begin{aligned} M_{AB}^{00} &= \begin{bmatrix} 1 & 0 & 0 \\ 0 & 0 & 0 \\ 0 & 0 & 0 \end{bmatrix} \\ M_{AB}^{10} &= \begin{bmatrix} 0 \\ \psi_1(h, q) \end{bmatrix} [0 \ \psi_1(h, q)^*], \quad \psi_1(h, q) = \frac{1}{\sqrt{2}} \begin{bmatrix} \sin 2h + i \sin 2(h - q) \\ \cos 2h - i \cos 2(h - q) \end{bmatrix} \\ M_{AB}^{01} &= \begin{bmatrix} 0 \\ \psi_2(h, q) \end{bmatrix} [0 \ \psi_2(h, q)^*], \quad \psi_2(h, q) = \frac{1}{\sqrt{2}} \begin{bmatrix} \cos 2h + i \cos 2(h - q) \\ -\sin 2h + i \sin 2(h - q) \end{bmatrix} \end{aligned} \quad (46)$$

A similar set of projectors can be written for C and D with the variables h, q replaced by their primed counterparts h', q' .

The protocol is to measure the probabilities for enough settings of the variables that the elements of the two-photon density operator can be estimated. The two-photon density operator is the direct product of the one-photon density operator, for which the set of 3 states given above forms a basis. The basis states of the two-photon (9×9) density operator, ρ , are: $|ijk\ell\rangle = |i\rangle_e|j\rangle_f|k\rangle_g|\ell\rangle_h$ with $i, j, k, \ell \in \{0, 1\}$. Hence,

$$\begin{aligned} \text{zero photon} & \quad |0000\rangle \\ \text{one photon} & \quad |0100\rangle, |1000\rangle, |0001\rangle, |0010\rangle \\ \text{two photon} & \quad |0101\rangle, |0110\rangle, |1001\rangle, |1010\rangle \end{aligned}$$

simulation results: one-arm

Consider only one arm of the apparatus in figure 2, say the upper arm with detectors (A,B). Suppose the wave plate settings are,

$$\{ h_\gamma, q_\gamma \mid \gamma = 1, \dots, n_{\text{cfg}} \} \quad (47)$$

Assume also that the incoming state *always* is one photon, never none. Hence, $\rho \in \mathbb{C}^{2 \times 2}$ and the projectors are:

$$\begin{aligned} M_\gamma^{10} &= \psi_1(h_\gamma, q_\gamma) \psi_1(h_\gamma, q_\gamma)^* \\ M_\gamma^{01} &= \psi_2(h_\gamma, q_\gamma) \psi_2(h_\gamma, q_\gamma)^* \end{aligned} \quad (48)$$

with ψ_1, ψ_2 from (46). Assuming each detector has efficiency η , $0 \leq \eta \leq 1$ and a non-zero dark count probability, δ , $0 \leq \delta \leq 1$, then there are four possible outcomes at detectors A,B given in the following table:

α	A	B
10	1	0
01	0	1
00	0	0
11	1	1

Following [15, 39] the probability of a dark count is denoted by the conditional probability,

$$\nu_{1|0} = \delta \quad (49)$$

where $1|0$ means the detector has fired “1” given that no photon is present at the detector “0.” As shown in [15], it therefore follows that the probability that the detector does not fire “0” although a photon is present at the detector “1” is given by,

$$\nu_{0|1} = (1 - \eta)(1 - \delta) \quad (50)$$

Here $1 - \eta$ is the probability of no detection and $1 - \delta$ is the probability of no dark count. The remaining conditional probabilities are, by definition, constrained to obey:

$$\begin{aligned} \nu_{1|0} + \nu_{0|0} &= 1 \\ \nu_{1|1} + \nu_{0|1} &= 1 \end{aligned} \quad (51)$$

The probabilities for the firing patterns in the above table are thus given by (7) with the following observables $M_{\alpha\gamma}$:

$$\begin{aligned} M_{10,\gamma} &= \nu_{1|1}\nu_{0|0}M_\gamma^{10} + \nu_{1|0}\nu_{0|1}M_\gamma^{01} \\ M_{01,\gamma} &= \nu_{0|1}\nu_{1|0}M_\gamma^{10} + \nu_{0|0}\nu_{1|1}M_\gamma^{01} \\ M_{00,\gamma} &= \nu_{0|1}\nu_{0|0}M_\gamma^{10} + \nu_{0|0}\nu_{0|1}M_\gamma^{01} \\ M_{11,\gamma} &= \nu_{1|1}\nu_{1|0}M_\gamma^{10} + \nu_{1|0}\nu_{1|1}M_\gamma^{01} \end{aligned} \quad (52)$$

Numerical computer simulations were performed for two input state cases:

$$\begin{aligned}
\textbf{pure state:} \quad \rho_{\text{pure}} &= \frac{1}{2} \begin{bmatrix} 1 & 1 \\ 1 & 1 \end{bmatrix} = \psi_0 \psi_0^*, \quad \psi_0 = \frac{1}{\sqrt{2}} \begin{bmatrix} 1 \\ 1 \end{bmatrix} \\
\textbf{mixed state:} \quad \rho_{\text{mixd}} &= \begin{bmatrix} 0.6 & -0.2i \\ 0.2i & 0.4 \end{bmatrix}
\end{aligned} \tag{53}$$

For each input state case we computed λ^{opt} with and without “noise:”

$$\begin{aligned}
\text{no noise} \quad & \begin{cases} \text{detector efficiency} & \eta = 1 \\ \text{dark count probability} & \delta = 0 \end{cases} \\
\text{yes noise} \quad & \begin{cases} \text{detector efficiency} & \eta = 0.75 \\ \text{dark count probability} & \delta = 0.05 \end{cases}
\end{aligned} \tag{54}$$

For all cases and noise conditions we used the wave plate settings:

$$\begin{aligned}
h_i &= (i-1)(5^\circ), \quad i = 1, \dots, 10 \\
q_i &= (i-1)(5^\circ), \quad i = 1, \dots, 10
\end{aligned} \tag{55}$$

Both angles are set from 0 to 45° in 5° increments. This yields a total of $n_{\text{cfg}} = 10^2 = 100$ configurations corresponding to all the wave plate combinations.

Figure 3 shows the optimal distributions λ^{opt} versus configurations $\gamma = 1, \dots, 100$ for all four test cases: two input states with and without noise. Observe that the optimal distributions are *not* uniform but are concentrated near the same particular wave plate settings. These settings are very close to those established in [17].

To check the gap between the relaxed optimum λ^{opt} and the unknown integer optimum we appeal to (36)-(37). The following table shows that these distributions are good approximation to the unknown optimal integer solution for even not so large ℓ_{expt} for the two state cases with no noise. Similar results were obtained for the noisy case.

ℓ_{expt}	$\frac{V(\ell_{\text{expt}} \lambda_{\text{pure}}^{\text{opt}}, \rho_{\text{pure}})}{V(\ell_{\text{expt}}^{\text{round}}(\rho_{\text{pure}}), \rho_{\text{pure}})}$	$\frac{V(\ell_{\text{expt}} \lambda_{\text{mixd}}^{\text{opt}}, \rho_{\text{mixd}})}{V(\ell_{\text{expt}}^{\text{round}}(\rho_{\text{mixd}}), \rho_{\text{mixd}})}$
100	.9797	.7761
1000	.9950	.9735
10,000	.9989	.9954

The following table compares the distributions for optimal, suboptimal with 8 angles, uniform at the 8 suboptimal angles, and uniform at all 100 angles by computing the minimum number

of experiments required to obtain an RMS estimation error of no more than 0.01.

input state	optimal round $\{\ell_{\text{expt}}\lambda^{\text{opt}}\}$ $n_{\text{cfg}} = 100$	suboptimal round $\{\ell_{\text{expt}}\lambda^{\text{sub}}\}$ $n_{\text{cfg}} = 8$	uniform $(1/8) \mathbf{1}(\lambda^{\text{sub}})$ $n_{\text{cfg}} = 8$	uniform $(1/100) \mathbf{1}(\lambda^{\text{opt}})$ $n_{\text{cfg}} = 100$
ρ_{pure} , no noise	20, 308	20, 308	20, 638	29, 274
ρ_{pure} , yes noise	37, 775	64, 129	40, 178	52, 825
ρ_{mixd} , no noise	41, 890	92, 471	69, 750	64, 780
ρ_{mixd} , yes noise	61, 049	134, 918	101, 425	94, 385

For these optical experiments there is significant cost (in time) associated with changing wave plate angles and very little cost (in time) for an experiment. As a result, although the uniform distribution at all 100 angles does not require a significant increase in the number of experiments, and in some cases fewer experiments than the suboptimal case, it is *very* costly in terms of changing wave plate angles. The following table shows the wave plate settings and suboptimal distributions from the above table.

h	q	$\lambda^{\text{sub}}(\rho_{\text{pure}})$ no noise	$\lambda^{\text{sub}}(\rho_{\text{pure}})$ yes noise	$\lambda^{\text{sub}}(\rho_{\text{mixd}})$ no noise	$\lambda^{\text{sub}}(\rho_{\text{mixd}})$ yes noise
0	0	0.24	0.23	0.14	0.14
5	0	0	0.11	0.11	0.11
10	0	0	0.04	0	0
15	45	0	0	0.07	0.07
20	40	0.01	0	0	0
20	45	0.25	0.12	0.19	0.19
25	45	0.25	0.13	0.21	0.21
30	45	0	0	0.07	0.07
35	0	0	0.04	0	0
40	0	0	0.09	0.07	0.07
45	0	0.24	0.23	0.14	0.14
45	5	0	0	0	0

This table shows that only a few wave plate angle changes are necessary if the suboptimal distributions are invoked. And from the previous table, as already observed, the suboptimal settings do not require a significant increase in the number of experiments required to achieve the desired estimation accuracy.

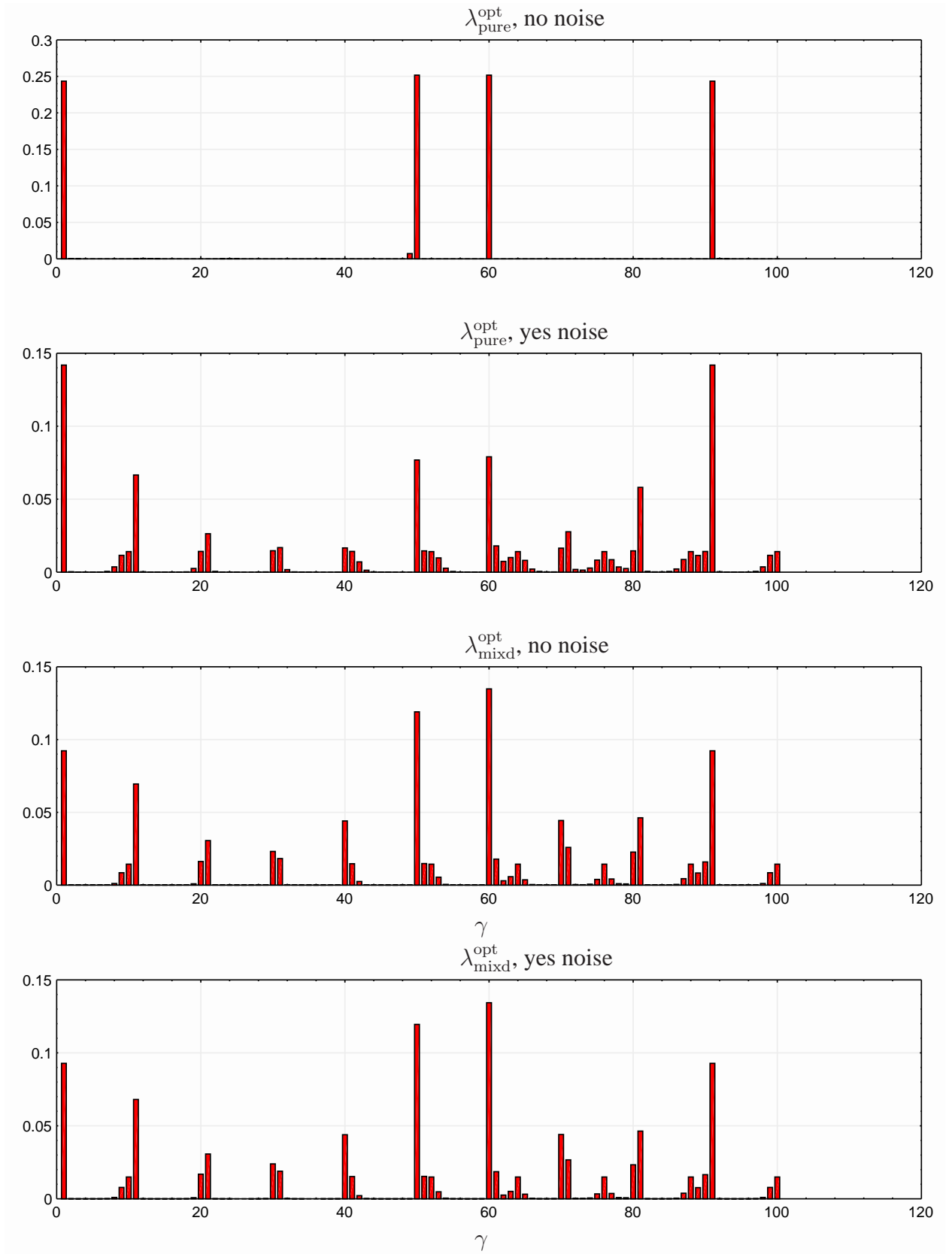


Figure 3: optimal distributions – one-arm

simulation results: both arms

We explore the two arm case under the assumption that two photons are always present at the input, thereby excluding the zero photon case.⁶ The table of detector firing patterns is:

α	A	B	C	D
0101	0	1	0	1
0110	0	1	1	0
1001	1	0	0	1
1010	1	0	1	0

The following three 4×4 input states are considered:

$$\begin{aligned}
&\rho_{\text{pure}} \otimes \rho_{\text{pure}} \\
&\rho_{\text{pure}} \otimes \rho_{\text{mixd}} \\
&\rho_{\text{mixd}} \otimes \rho_{\text{mixd}}
\end{aligned} \tag{56}$$

with ρ_{pure} , ρ_{mixd} given by (53). We use the angles from the one-arm optimal distribution for the largest 8 values:

$$\begin{aligned}
h &\in [0, 20, 25, 45] & q &\in [0, 20, 25, 45] \\
h' &\in [0, 20, 25, 45] & q' &\in [0, 20, 25, 45]
\end{aligned} \tag{57}$$

This yields a total of $n_{\text{cfg}} = 4^4 = 256$ wave plate settings.

Figure 4 shows the optimal distributions λ^{opt} versus configurations $\gamma = 1, \dots, 256$ for all three input states. In this case the optimal distributions λ^{opt} are nearly uniform in magnitude. The following table compares the distributions for optimal, suboptimal with 25 angles, uniform at the 25 suboptimal angles, and uniform at all 256 angles by examining the minimum number of experiments required to obtain an RMS estimation error of no more than 0.01.

input state	optimal round $\{\ell_{\text{expt}} \lambda^{\text{opt}}\}$ $n_{\text{cfg}} = 256$	suboptimal round $\{\ell_{\text{expt}} \lambda^{\text{sub}}\}$ $n_{\text{cfg}} = 25$	uniform (1/25) $\mathbf{1}(\lambda^{\text{sub}})$ $n_{\text{cfg}} = 25$	uniform (1/256) $\mathbf{1}(\lambda^{\text{opt}})$ $n_{\text{cfg}} = 256$
$\rho_{\text{pure}} \otimes \rho_{\text{pure}}$	81, 870	81, 877	86, 942	115, 165
$\rho_{\text{pure}} \otimes \rho_{\text{mixd}}$	135, 158	139, 151	156, 219	226, 234
$\rho_{\text{mixd}} \otimes \rho_{\text{mixd}}$	225, 739	288, 163	262, 833	427, 292

As might be expected it is easier to estimate all pure states than mixed states. The table also shows that the optimal solution can be used effectively to guide the selection of suboptimal distributions.

⁶In an actual laboratory setting it is important to include the zero photon case; it is often that no photon is actually present at the input.

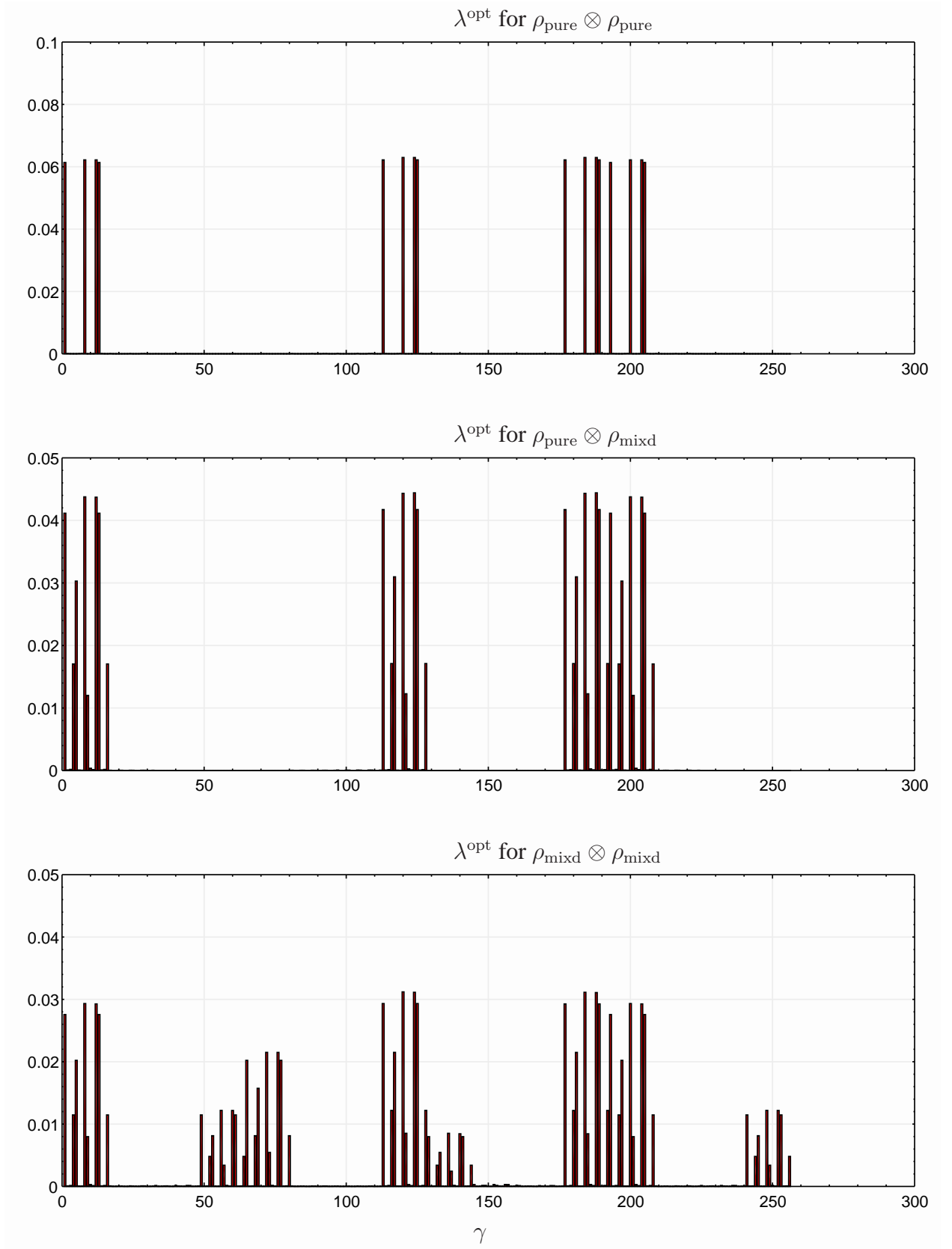


Figure 4: optimal distributions – two-arms

2.5 Maximum likelihood state distribution estimation

A variation on the state estimation problem is to estimate the *distribution* of a known set of input states. The set-up for data collection is shown schematically in Figure 5 for configuration γ .

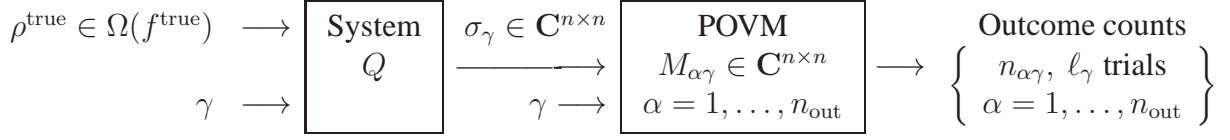


Figure 5: System/POVM.

In this case the input state ρ^{true} is drawn from,

$$\Omega(f^{\text{true}}) = \left\{ \rho(i), f^{\text{true}}(i) \mid i = 1, \dots, n_{\text{in}} \right\} \quad (58)$$

which consists of a set of known states, $\{\rho(1), \dots, \rho(n_{\text{in}})\}$, with corresponding unknown occurrence probabilities $f^{\text{true}} = \{f^{\text{true}}(1), \dots, f^{\text{true}}(n_{\text{in}})\}$ where $0 \leq f^{\text{true}}(i) \leq 1, \forall i$ and $\sum_i f^{\text{true}}(i) = 1$. The objective is to use the data and knowledge of the input state set to estimate the vector of occurrence probabilities f^{true} . Proceeding as before, assume that the input state *model* is $\rho \in \Omega(f)$ where $\Omega(f) = \{\rho(i), f(i) \mid i = 1, \dots, n_{\text{in}}\}$ and where the vector of distributions $f = [f(1), \dots, f(n_{\text{in}})]^T \in \mathbf{R}^{n_{\text{in}}}$ is to be estimated. In this case the input state can be represented by the mixed state,

$$\rho(f) = \sum_{i=1}^{n_{\text{in}}} f(i) \rho(i) \quad (59)$$

The ML estimate of f is then the solution of the optimization problem:

$$\begin{aligned} & \text{minimize} && L(f) = - \sum_{\alpha, \gamma} n_{\alpha\gamma} \log \text{Tr } O_{\alpha\gamma} \rho(f) \\ & \text{subject to} && \sum_{i=1}^{n_{\text{in}}} f(i) = 1, \quad f(i) \geq 0, \quad i = 1, \dots, n_{\text{in}} \end{aligned} \quad (60)$$

As in the MLE for quantum state estimation (17), the objective is log-convex in the state $\rho(f)$, the state is linear in $f \in \mathbf{R}^{n_{\text{in}}}$, and the constraints form a convex set in f . Hence, this is a convex optimization problem in the variable f . Combining (59) with (60) gives the more explicit form,

$$\begin{aligned} & \text{minimize} && L(f) = - \sum_{\alpha, \gamma} n_{\alpha\gamma} \log a_{\alpha\gamma}^T f \\ & \text{subject to} && \sum_{i=1}^{n_{\text{in}}} f(i) = 1, \quad f(i) \geq 0, \quad i = 1, \dots, n_{\text{in}} \\ & && a_{\alpha\gamma} = [\text{Tr } O_{\alpha\gamma} \rho(1) \cdots \text{Tr } O_{\alpha\gamma} \rho(n_{\text{in}})]^T \in \mathbf{R}^{n_{\text{in}}}, \quad \forall \alpha, \gamma \end{aligned} \quad (61)$$

Here again as in (25) we could solve for f using the empirical estimate of the outcome probabilities as in (26):

$$\begin{aligned} & \text{minimize} && \sum_{\alpha, \gamma} w_\gamma \left(p_{\alpha\gamma}^{\text{emp}} - a_{\alpha\gamma}^T f \right)^2 \\ & \text{subject to} && \sum_{i=1}^{n_{\text{in}}} f(i) = 1, \quad f(i) \geq 0, \quad i = 1, \dots, n_{\text{in}} \end{aligned} \quad (62)$$

2.6 Experiment design for state distribution estimation

Let $f^{\text{surr}} \in \mathbf{R}^{n_{\text{in}}}$ be a surrogate for the true state distribution, f^{true} . Following the derivation of (28) in Appendix §A.3, the associated (relaxed) optimal experiment design problem is,

$$\begin{aligned} & \text{minimize} && V(\lambda, f^{\text{surr}}) = \text{Tr} \left(\sum_{\gamma} \lambda_{\gamma} G_{\gamma}(f^{\text{surr}}) \right)^{-1} \\ & \text{subject to} && \sum_{\gamma} \lambda_{\gamma} = 1 \\ & && \lambda_{\gamma} \geq 0, \gamma = 1, \dots, n_{\text{cfg}} \end{aligned} \quad (63)$$

where

$$G_{\gamma}(f^{\text{surr}}) = C_{\text{eq}}^T \left(\sum_{\alpha} \frac{a_{\alpha\gamma} a_{\alpha\gamma}^T}{p_{\alpha\gamma}(f^{\text{surr}})} \right) C_{\text{eq}} \in \mathbf{R}^{n_{\text{in}}-1 \times n_{\text{in}}-1} \quad (64)$$

with $a_{\alpha\gamma} \in \mathbf{R}^{n_{\text{in}}}$ from (60) and where $C_{\text{eq}} \in \mathbf{R}^{n_{\text{in}} \times n_{\text{in}}-1}$ is part of the unitary matrix W in the singular value decomposition: $1_{n_{\text{in}}}^T = U S W^T$, $W = [C_{\text{eq}}] \in \mathbf{R}^{n_{\text{in}} \times n_{\text{in}}}$.

3 Quantum Process Tomography: OSR Estimation

We explore two methods of identification for determining the Q -system from data: (i) in this section, estimating the OSR in a fixed basis, and (ii) in Section §4, estimating Hamiltonian parameters. In either case, the set-up is now as shown in Figure 6.

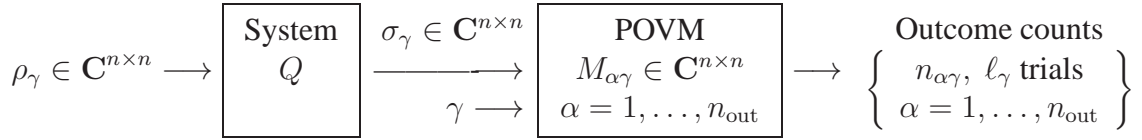


Figure 6: System/POVM.

The main difference between state tomography (Figure 1) and process tomography (Figure 6) is that in the latter case the input state is prepared at specific values, ρ_{γ} , depending on the configuration, whereas the Q -system does not depend on the configuration. If the process varies with every change in configuration it would be much more difficult to estimate; a model of configuration dependence would need to be established. This situation is perhaps amenable with Hamiltonian parameter estimation but will not be pursued here.

3.1 Maximum likelihood OSR estimation

As already stated, the Krause matrices for modeling the (trace preserving) Q -system in this case are *not* dependent on the configuration γ , specifically, $K = \{ K_k \mid k = 1, \dots, \kappa \}$ with $\kappa \leq n^2$. Using (10), the reduced state model in Figure 6 as a function of K is,

$$\sigma_{\gamma}(K) = Q(\rho_{\gamma}, K) = \sum_{k=1}^{\kappa} K_k \rho_{\gamma} K_k^*, \quad \sum_{k=1}^{\kappa} K_k^* K_k = I_n \quad (65)$$

Combining the above with the measurement model (9) gives the probability outcomes model,

$$p_{\alpha\gamma}(K) = \text{Tr } O_{\alpha\gamma}(K)\rho_\gamma, \quad O_{\alpha\gamma}(K) = \sum_{k=1}^{\kappa} K_k^* M_{\alpha\gamma} K_k \quad (66)$$

The log-likelihood function (16) is,

$$L(D, K) = - \sum_{\alpha, \gamma} n_{\alpha\gamma} \log \text{Tr } O_{\alpha\gamma}(K)\rho_\gamma \quad (67)$$

An ML estimate of K is then a solution to,

$$\begin{aligned} &\text{minimize} && L(D, K) = - \sum_{\alpha, \gamma} n_{\alpha\gamma} \log \text{Tr } \sum_{k=1}^{\kappa} K_k^* M_{\alpha\gamma} K_k \rho_\gamma \\ &\text{subject to} && \sum_{k=1}^{\kappa} K_k^* K_k = I_n \end{aligned} \quad (68)$$

This is not a convex optimization for two reasons: the equality constraint is not linear in K and the objective function is not convex. The problem can be transformed – more accurately, embedded – into a convex optimization problem by expanding the Kraus matrices in a fixed basis. The procedure, described in [27, §8.4.2], is as follows: since any matrix in $\mathbf{C}^{n \times n}$ can be represented by n^2 complex numbers, let

$$\left\{ B_i \in \mathbf{C}^{n \times n} \mid i = 1, \dots, n^2 \right\} \quad (69)$$

be a basis for matrices in $\mathbf{C}^{n \times n}$. The Kraus matrices can thus be expressed as,

$$K_k = \sum_{i=1}^{n^2} a_{ki} B_i, \quad k = 1, \dots, \kappa \quad (70)$$

where the n^2 coefficients $\{a_{ki}\}$ are complex scalars. Introduce the matrix $X \in \mathbf{C}^{n^2 \times n^2}$, often referred to as the *superoperator*, with elements,

$$X_{ij} = \sum_{k=1}^{\kappa} a_{ki}^* a_{kj}, \quad i, j = 1, \dots, n^2 \quad (71)$$

As shown in [27], from the requirement to preserve probability, X is restricted to the convex set,

$$X \geq 0, \quad \sum_{i,j=1}^{n^2} X_{ij} B_i^* B_j = I_n \quad (72)$$

The system output state (65) and outcome probabilities (66) now become,

$$\sigma_\gamma(X) = Q(\rho_\gamma, X) = \sum_{i,j=1}^{n^2} X_{ij} B_i \rho_\gamma B_j^* \quad (73)$$

$$p_{\alpha\gamma}(X) = \text{Tr } O_{\alpha\gamma} Q(\rho_\gamma, X) = \text{Tr } X R_{\alpha\gamma}$$

where the matrix $R_{\alpha\gamma} \in \mathbf{C}^{n^2 \times n^2}$ has elements,

$$[R_{\alpha\gamma}]_{ij} = \text{Tr } B_j \rho_\gamma B_i^* O_{\alpha\gamma}, \quad i, j = 1, \dots, n^2 \quad (74)$$

Quantum process tomography is then estimating $X \in \mathbb{C}^{n^2 \times n^2}$ from the data set D (4). An ML estimate is obtained by solving for X from:

$$\begin{aligned} & \text{minimize} && L(D, X) = -\sum_{\alpha, \gamma} n_{\alpha\gamma} \log \text{Tr } X R_{\alpha\gamma} \\ & \text{subject to} && X \geq 0, \quad \sum_{ij} X_{ij} B_i^* B_j = I_n \end{aligned} \quad (75)$$

This problem has essentially the same form as (17), and hence is also a convex optimization problem with the optimization variables being the elements of the matrix X . Since $X = X^* \in \mathbb{C}^{n^2 \times n^2}$, it can be parametrized by n^4 real variables. Accounting for the n^2 real linear equality constraints, the number of free (real) variables in X is thus $n^4 - n^2$. This can be quite large even for a relatively small number of qubits, *e.g.*, for $q = [1, 2, 3, 4]$ qubits, $n = 2^q = [2, 4, 8, 16]$ and $n^4 - n^2 = [12, 240, 4032, 65280]$. This exponential (in qubit) growth is the main drawback to using this approach.

The X (superoperator) matrix can be transformed back to Kraus operators via the singular value decomposition [27, §8.4.2]. Specifically, let $X = V S V^*$ with unitary $V \in \mathbb{C}^{n^2 \times n^2}$ and $S = \text{diag}(s_1 \cdots s_{n^2})$ with the singular values ordered so that $s_1 \geq s_2 \geq \cdots \geq s_{n^2} \geq 0$. Then the coefficients in the basis representation of the Kraus matrices (70) are,

$$a_{ki} = \sqrt{s_k} V_{ik}^*, \quad k, i = 1, \dots, n^2 \quad (76)$$

Theoretically there can be fewer than n^2 Kraus operators. For example, if the Q system is unitary, then,

$$Q(\rho) = U \rho U^* \quad (77)$$

In effect, there is one Kraus operator, U , which is unitary and of the same dimension as the input state ρ . The corresponding X matrix is a dyad, hence $\text{rank } X = 1$. A rank constraint is not convex. However, the X matrix is symmetric and positive semidefinite, so the heuristic from [10] applies where the rank constraint is replaced by the trace constraint,

$$\text{Tr } X \leq \eta \quad (78)$$

From the singular value decomposition of X , $\text{Tr } X = \sum_k s_k$, and hence, adding the constraint (78) to (75) will force some (or many) of the s_k to be small which can be eliminated (post-optimization) thereby reducing the rank. The auxiliary parameter η can be used to find a tradeoff between simpler realizations and performance. The estimation problem is then:

$$\begin{aligned} & \text{minimize} && L(D, X) = -\sum_{\alpha, \gamma} n_{\alpha\gamma} \log \text{Tr } X R_{\alpha\gamma} \\ & \text{subject to} && X \geq 0, \quad \sum_{ij} X_{ij} B_i^* B_j = I_n \\ & && \text{Tr } X \leq \eta \end{aligned} \quad (79)$$

3.2 Experiment design for OSR estimation

Let $X^{\text{surr}} \in \mathbb{C}^{n^2 \times n^2}$ be a surrogate for the true OSR, X^{true} . As derived in Appendix §A.4, the associated (relaxed) optimal experiment design problem is,

$$\begin{aligned} & \text{minimize} && V(\lambda, X^{\text{surr}}) = \text{Tr} \left(\sum_{\gamma} \lambda_{\gamma} G_{\gamma}(X^{\text{surr}}) \right)^{-1} \\ & \text{subject to} && \sum_{\gamma} \lambda_{\gamma} = 1 \\ & && \lambda_{\gamma} \geq 0, \quad \gamma = 1, \dots, n_{\text{cfg}} \end{aligned} \quad (80)$$

where

$$G_\gamma(X^{\text{surr}}) = C_{\text{eq}}^* \left(\sum_\alpha \frac{a_{\alpha\gamma} a_{\alpha\gamma}^*}{p_{\alpha\gamma}(X^{\text{surr}})} \right) C_{\text{eq}} \quad (81)$$

$$a_{\alpha\gamma} = \text{vec } R_{\alpha\gamma} \in \mathbb{C}^{n^4}$$

and $C_{\text{eq}} \in \mathbb{C}^{n^4 \times n^4 - n^2}$ is part of the unitary matrix $W = [C \ C_{\text{eq}}] \in \mathbb{C}^{n^4 \times n^4}$ in the singular value decomposition of the $n^2 \times n^4$ matrix,

$$[a_1 \ \cdots \ a_{n^4}] = U \begin{bmatrix} \sqrt{n} I_{n^2} & 0_{n^2 \times n^4 - n^2} \end{bmatrix} W^* \quad (82)$$

with $a_k = \text{vec}(B_i^* B_j) \in \mathbb{C}^{n^2}$ for $k = i + (j - 1)n^2$, $i, j = 1, \dots, n^2$. The columns of C_{eq} , *i.e.*, the last $n^4 - n^2$ columns of W , are a basis for the nullspace of $[a_1 \ \cdots \ a_{n^4}]$.

3.3 Example: experiment design for OSR estimation

Consider the POVM set from the one-arm photon detector (§2.4) using all combinations of the following set wave-plate angles,

$$h = [0 \ 30 \ 45], \ q = [0 \ 30 \ 45]$$

Assume detector efficiency $\eta = 0.75$ and dark count probability $\delta = 0.05$. The set of inputs (state configurations) is

$$|0\rangle, |1\rangle, |+\rangle = (|0\rangle + |1\rangle)/\sqrt{2}, \ |-\rangle = (|0\rangle + i|1\rangle)/\sqrt{2}$$

The 9 combinations of angles together with the 4 combinations of input states gives a total of 36 configurations, $\gamma = 1, \dots, n_{\text{cfg}} = 36$.

Figure 7 shows the optimal distribution of experiments for the 36 configurations using the true OSR corresponding to the Pauli basis set $\{I_2/\sqrt{2}, \sigma_x/\sqrt{2}, \sigma_y/\sqrt{2}, \sigma_z/\sqrt{2}\}$. Since the system is simply the identity, $Q(\rho) = \rho$, with this basis choice, $X^{\text{true}} = \text{diag}(2 \ 0 \ 0 \ 0)$. (No knowledge of the system being identity is used, hence, all elements of X^{true} are estimated, not just the single element in the “11” location.)

The following table displays the minimum number of experiments required to meet estimation accuracies of 0.05 and 0.01 for both uniform and optimal distributions.

accuracy	λ^{opt}	λ^{unif}
0.01	856,676	1,304,561
0.05	34,268	52,183

Approximately 35% fewer experiments are needed using the optimal distribution. Although not dramatic, as in the photon estimation example §2.4, there is a large penalty, in terms of time, for changing wave-plate angles.

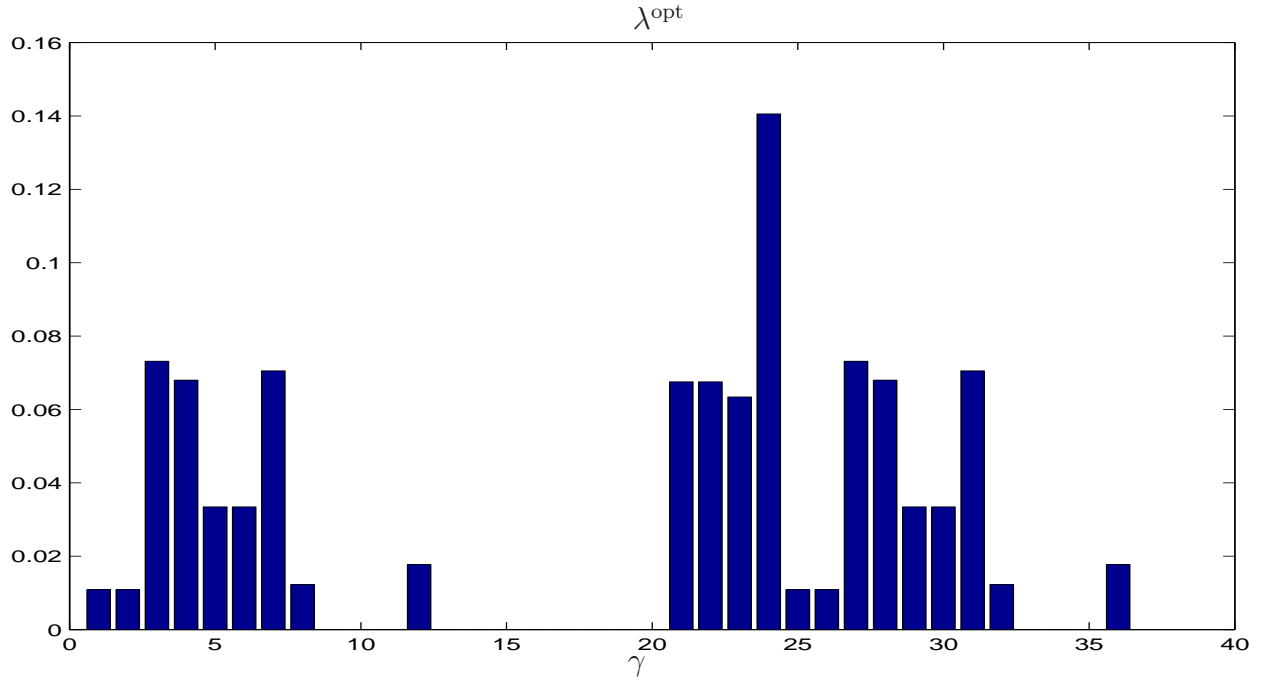


Figure 7: optimal distributions for OSR estimation

The following Table shows the 22 out of 36 configurations for $\lambda_{\gamma}^{\text{opt}} > 0.01$.

γ	$\lambda_{\gamma}^{\text{opt}}$	h_{γ}	q_{γ}	ρ_{γ}
1	0.011	0	0	$ 0\rangle$
2	0.011	0	0	$ 1\rangle$
3	0.073	0	0	$ +\rangle$
4	0.068	0	0	$ -\rangle$
5	0.033	0	30	$ 0\rangle$
6	0.033	0	30	$ 1\rangle$
7	0.071	0	30	$ +\rangle$
8	0.012	0	30	$ -\rangle$
12	0.018	0	45	$ -\rangle$
21	0.068	30	45	$ 0\rangle$
22	0.068	30	45	$ 1\rangle$
23	0.063	30	45	$ +\rangle$
24	0.141	30	45	$ -\rangle$
25	0.011	45	0	$ 0\rangle$
26	0.011	45	0	$ 1\rangle$
27	0.073	45	0	$ +\rangle$
28	0.068	45	0	$ -\rangle$
29	0.033	45	30	$ 0\rangle$
30	0.033	45	30	$ 1\rangle$
31	0.071	45	30	$ +\rangle$
32	0.012	45	30	$ -\rangle$
36	0.018	45	45	$ -\rangle$

3.4 Maximum likelihood OSR distribution estimation

Suppose the Kraus matrices are known up to a scale factor which is related to its probability of occurrence, that is,

$$\begin{aligned} K_k &= \sqrt{q_k} \bar{K}_k & \sum_{k=1}^{\kappa} q_k \bar{K}_k^* \bar{K}_k &= I_n \\ \sum_{k=1}^{\kappa} q_k &= 1 & q_k &\geq 0 \end{aligned} \quad k = 1, \dots, \kappa \quad (83)$$

One interpretation of this system model is that one of the matrices, say \bar{K}_1 , is the nominal (unperturbed) system, and the others, $\bar{K}_k, k = 2, \dots, \kappa$, are perturbations, each of them occurring with probability q_k . Examples of perturbations include the typical errors which can be handled by quantum error correction codes, *e.g.*, depolarization, phase damping, phase and bit flip; see, *e.g.*, [27, Ch.8].

The goal is to use the data to estimate the unknown vector of probabilities, $q = [q_1 \cdots q_{\kappa}]^T \in \mathbf{R}^{\kappa}$. Using the system model (83), the model probability outcomes are,

$$\begin{aligned} p_{\alpha\gamma} &= \text{Tr } M_{\alpha\gamma} \sum_{k=1}^{\kappa} q_k \bar{K}_k \rho_{\gamma} \bar{K}_k^* = a_{\alpha\gamma}^T q \\ a_{\alpha\gamma} &= \left[\text{Tr } M_{\alpha\gamma} \bar{K}_1 \rho_{\gamma} \bar{K}_1^* \cdots \text{Tr } M_{\alpha\gamma} \bar{K}_{\kappa} \rho_{\gamma} \bar{K}_{\kappa}^* \right]^T \in \mathbf{R}^{\kappa} \end{aligned} \quad (84)$$

The ML estimate of $q \in \mathbf{R}^{\kappa}$ is the solution of the optimization problem,

$$\begin{aligned} \text{minimize} \quad & L(q) = -\sum_{\alpha,\gamma} n_{\alpha\gamma} \log a_{\alpha\gamma}^T q \\ \text{subject to} \quad & \sum_{k=1}^{\kappa} q_k = 1, \quad q_k \geq 0, \quad k = 1, \dots, \kappa \end{aligned} \quad (85)$$

This is a convex optimization problem and is essentially in the same form as problem (60) which seeks the ML estimate of the input state distribution.

3.5 Experiment design for OSR distribution estimation

The formulation here is directly analogous to that of experiment design for state distribution estimation §2.6. Let $q^{\text{surr}} \in \mathbf{R}^{n_{\text{in}}}$ be a surrogate for the true OSR distribution, q^{true} . Following the lines of the derivation in Appendix §A.4, the associated (relaxed) optimal experiment design problem is,

$$\begin{aligned} \text{minimize} \quad & V(\lambda, q^{\text{surr}}) = \text{Tr} \left(\sum_{\gamma} \lambda_{\gamma} G_{\gamma}(q^{\text{surr}}) \right)^{-1} \\ \text{subject to} \quad & \sum_{\gamma} \lambda_{\gamma} = 1 \\ & \lambda_{\gamma} \geq 0, \quad \gamma = 1, \dots, n_{\text{cfg}} \end{aligned} \quad (86)$$

where

$$G_{\gamma}(q^{\text{surr}}) = C_{\text{eq}}^T \left(\sum_{\alpha} \frac{a_{\alpha\gamma} a_{\alpha\gamma}^T}{p_{\alpha\gamma}(q^{\text{surr}})} \right) C_{\text{eq}} \in \mathbf{R}^{n_{\text{in}}-1 \times n_{\text{in}}-1} \quad (87)$$

with $a_{\alpha\gamma} \in \mathbf{R}^{n_{\text{in}}}$ from (85) and where $C_{\text{eq}} \in \mathbf{R}^{n_{\text{in}} \times n_{\text{in}}-1}$ is part of the unitary matrix W in the singular value decomposition: $1_{n_{\text{in}}}^T = U S W^T$, $W = [C_{\text{eq}}] \in \mathbf{R}^{n_{\text{in}} \times n_{\text{in}}}$.

3.6 Example: experiment design for OSR distribution estimation

Consider a quantum process, or channel, where a single qubit state, $\rho \in \mathbb{C}^{2 \times 2}$, is corrupted by a *bit-flip error* with occurrence probability q_B and a *depolarizing error* with occurrence probability q_D . The process is described by the quantum operation,⁷

$$\begin{aligned} Q(\rho, q) &= q_I \rho + q_B X \rho X + q_D I/2 \\ q_I + q_B + q_D &= 1 \end{aligned} \quad (88)$$

where $q_I = 1 - (q_B + q_D)$ is the probability of no error occurring. The probability of observing outcome α with the system in configuration γ is,⁸

$$\begin{aligned} p_{\alpha\gamma}(q) &= \text{Tr } M_{\alpha\gamma} Q(\rho_\gamma, q) \\ &= \begin{bmatrix} \text{Tr } M_{\alpha\gamma} \rho_\gamma & \text{Tr } M_{\alpha\gamma} X \rho_\gamma X & \text{Tr } M_{\alpha\gamma} I/2 \end{bmatrix} \begin{bmatrix} q_I \\ q_B \\ q_D \end{bmatrix} \\ &= a_{\alpha\gamma}^T q \end{aligned} \quad (89)$$

An interesting aspect of this problem is that not all input states ρ_γ lead to identifiability of the occurrence probabilities. And this is independent of the choice of POVM $M_{\alpha\gamma}$. To see this consider the single pure input state,

$$\rho_\gamma = \psi\psi^*, \quad \psi = \begin{bmatrix} a \\ b \end{bmatrix}, \quad |a|^2 + |b|^2 = 1 \quad (90)$$

The output of the channel (88) is then,

$$Q(\psi\psi^*, q) = \begin{bmatrix} q_I|a|^2 + q_B|b|^2 + q_D/2 & q_Iab^* + q_Ba^*b \\ q_Ia^*b + q_Bab^* & q_I|b|^2 + q_B|a|^2 + q_D/2 \end{bmatrix} \quad (91)$$

Suppose we knew the elements of $Q(\psi\psi^*, q)$ perfectly; call them Q_{11}, Q_{12}, Q_{22} . Then in principal we could solve for the three occurrence probabilities from the linear system of equations,

$$\underbrace{\begin{bmatrix} |a|^2 & |b|^2 & 1/2 \\ |b|^2 & |a|^2 & 1/2 \\ ab^* & a^*b & 0 \end{bmatrix}}_R \begin{bmatrix} q_I \\ q_B \\ q_D \end{bmatrix} = \begin{bmatrix} Q_{11} \\ Q_{22} \\ Q_{12} \end{bmatrix} \quad (92)$$

If $\det R = 0$ then no unique solution exists; the occurrence probabilities are not *identifiable*. Specifically, $\det R = 0$ for all $a, b \in \mathbb{C}$ such that,

$$(\text{Re } ab^*)(|b|^2 - |a|^2) = 0, \quad |a|^2 + |b|^2 = 1 \quad (93)$$

⁷ X is one of the three 2×2 Pauli spin matrices: $X = \begin{bmatrix} 0 & 1 \\ 1 & 0 \end{bmatrix}$, $Y = \begin{bmatrix} 0 & -i \\ i & 0 \end{bmatrix}$, $Z = \begin{bmatrix} 1 & 0 \\ 0 & -1 \end{bmatrix}$

⁸As shown in [27, §8.3], an equivalent set of OSR elements which describe (88) are, $\sqrt{q_I} I$, $\sqrt{q_B} X$, $\sqrt{q_D} I/2$, $\sqrt{q_D} X/2$, $\sqrt{q_D} Y/2$, $\sqrt{q_D} Z/2$. Forming the probability outcomes in terms of this expansion results in an overparametrization.

Equivalently, $\det R = 0$ for the following sets of $a, b \in \mathbb{C}$:

$$(a = 0, |b| = 1), (|a| = 1, b = 0), (|a| = |b| = 1/\sqrt{2}) \quad (94)$$

Let the input state be a single pure state of the form

$$\psi(\theta) = \begin{bmatrix} \cos \theta \\ \sin \theta \end{bmatrix}, \quad (95)$$

Suppose the angle θ is restricted to the range $0 \leq \theta \leq 90^\circ$. Using (94), the occurrence probabilities are not identifiable for the angles θ . and respectively, the states $\psi(\theta)$, in the sets,

$$\theta \in \{0, 45^\circ, 90^\circ\}, \psi(\theta) \in \left\{ \begin{bmatrix} 1 \\ 0 \end{bmatrix}, \begin{bmatrix} 1/\sqrt{2} \\ 1/\sqrt{2} \end{bmatrix}, \begin{bmatrix} 0 \\ 1 \end{bmatrix} \right\} \quad (96)$$

Unfortunately, this excludes inputs identical to the computational basis states $|0\rangle$ or $|1\rangle$, respectively, $\psi(\theta)$ with $\theta = 0$ or $\theta = 90^\circ$.

We now solve the (relaxed) experiment design problem (86) for occurrence probabilities $(q_I, q_B, q_D) = (0.6, 0.2, 0.2)$ and with the POVM set given by (48). For illustrative purposes, we use only 16 of the 100 configurations represented by the wave plate angles (55). Specifically, the wave-plate angles are: $\{h = 0, 15, 30, 45\} \times \{q = 0, 15, 30, 45\}$. The optimization results are presented in the following table which shows the number of experiments per configuration (each of the 16 angle pairs) required to achieve an accuracy of 0.01 for the input states corresponding to the angles $\theta \in \{2, 10, 25, 35, 44\}$.

configurations		experiments per configuration				
h	q	$\theta = 2$	$\theta = 10$	$\theta = 25$	$\theta = 35$	$\theta = 44$
0	0	62,244	15,453	13,386	31,275	2,136,560
0	15	1	1	1	1	1
0	30	1	0	0	0	1
0	45	1	0	0	0	1
15	0	1	0	0	0	1
15	15	1	1	1	1	1
15	30	73,096	11,277	4,765	9,006	107,371
15	45	2,080,984	89,588	18,598	14,573	62,187
30	0	1	0	0	0	1
30	15	1	0	0	0	1
30	30	1	0	0	0	1
30	45	2,080,984	89,588	18,598	14,573	62,187
45	0	62,244	15,453	13,386	31,275	2,136,560
45	15	1	1	1	1	1
45	30	1	0	0	0	1
45	45	1	0	0	0	1
$\ell_{\text{expt}} =$		4,359,563	221,362	68,736	100,705	4,504,876

The numerical example shows that for input states close to those states which make the problem not identifiable (96), the number of experiments required to achieve the specified accuracy grows very large. In this case, $\theta = 2$ and $\theta = 44$ are close to the bad angles 0 and 45, and the number of experiments is quite large.

4 Hamiltonian Parameter Estimation

The process of modeling a quantum system in this case begins with the construction of a Hamiltonian *operator* on an infinite dimensional Hilbert space. *Eventually*, a finite dimensional approximation is invoked in order to calculate anything. (In some cases a finite dimensional model is immediately appropriate, *e.g.*, spin systems, [11, Ch.12-9].) The finite dimensional model is the starting point here.

4.1 Maximum likelihood Hamiltonian parameter estimation

The quantum system is modeled by a finite dimensional Hamiltonian matrix $H(t, \theta) \in \mathbb{C}^{n \times n}$, having a known dependence on time t , $0 \leq t \leq t_f$, and on an unknown parameter vector $\theta \in \mathbb{R}^{n_\theta}$. The model density matrix will depend on θ and the initial (prepared and known) state drawn from the set of states $\{\rho_\beta^{\text{init}} \in \mathbb{C}^{n \times n} \mid \beta = 1, \dots, n_{\text{in}}\}$. Thus, the density matrix associated with initial state ρ_β^{init} is $\rho_\beta(t, \theta) \in \mathbb{C}^{n \times n}$ which evolves according to,

$$i\hbar \dot{\rho}_\beta = [H(t, \theta), \rho_\beta], \quad \rho_\beta(0, \theta) = \rho_\beta^{\text{init}} \quad (97)$$

Equivalently,

$$\rho_\beta(t, \theta) = U(t, \theta) \rho_\beta^{\text{init}} U(t, \theta)^* \quad (98)$$

where $U(t, \theta) \in \mathbb{C}^{n \times n}$ is the unitary propagator associated with $H(t, \theta)$ which satisfies,

$$i\hbar \dot{U} = H(t, \theta)U, \quad U(0, \theta) = I_n \quad (99)$$

At each of n_{sa} sample times in a time interval of duration t_f , measurements are recorded from identical repeated experiments. Specifically, let $\{t_\tau \mid \tau = 1, \dots, n_{\text{sa}}\}$ denote the sample times relative to the start of each experiment. Let $n_{\alpha\beta\tau}$ be the number of times the outcome α is recorded at t_τ with initial state ρ_β^{init} from $\ell_{\beta\tau}$ experiments. The data set thus consists of all the outcome counts,

$$D = \{n_{\alpha\beta\tau} \mid \alpha = 1, \dots, n_{\text{out}}, \beta = 1, \dots, n_{\text{in}}, \tau = 1, \dots, n_{\text{sa}}\} \quad (100)$$

The *configurations* previously enumerated and labeled by $\gamma = 1, \dots, n_{\text{cfg}}$ are in this case all the combinations of input states ρ_β^{init} and sample times τ , thus $n_{\text{cfg}} = n_{\text{in}}n_{\text{sa}}$. For the POVM M_α , the model outcome probability per configuration pair $(\rho_\beta^{\text{init}}, t_\tau)$ is,

$$\begin{aligned} p_{\alpha\beta\tau}(\theta) &= \text{Tr } M_\alpha \rho_\beta(t_\tau, \theta) = \text{Tr } O_{\alpha\tau}(\theta) \rho_\beta^{\text{init}} \\ O_{\alpha\tau}(\theta) &= U(t_\tau, \theta)^* M_\alpha U(t_\tau, \theta) \end{aligned} \quad (101)$$

The Maximum Likelihood estimate, $\theta^{\text{ML}} \in \mathbb{R}^{n_\theta}$, is obtained as the solution to the optimization problem:

$$\begin{aligned} &\text{minimize} \quad L(D, \theta) = -\sum_{\alpha, \beta, \tau} n_{\alpha\beta\tau} \log \text{Tr } O_{\alpha\tau}(\theta) \rho_\beta^{\text{init}} \\ &\text{subject to} \quad \theta \in \Theta \end{aligned} \quad (102)$$

where Θ is a set of constraints on θ . For example, it may be known that θ is restricted to a region near a nominal value, *e.g.*, $\Theta = \{\theta \mid \|\theta - \theta_{\text{nom}}\| \leq \delta\}$. Although this latter set is convex, unfortunately, the likelihood function, $L(D, \theta)$, is not guaranteed to be convex in θ . It is possible, however, that it is convex in the restricted region Θ , for example, if δ is sufficiently small.

4.2 Experiment design for Hamiltonian parameter estimation

Despite the fact that Hamiltonian parameter estimation is not convex, the (relaxed) experiment design problem is convex. A direct application of the Cramér-Rao bound to the likelihood function in (102) results in the following.

Hamiltonian parameter estimation variance lower bound Suppose the system generating the data is in the model set used for estimation, *i.e.*, (13) holds. For $\ell = [\ell_1 \cdots \ell_{n_{\text{cfg}}}]$ experiments per configuration $(\rho_{\beta}^{\text{init}}, t_{\tau})$, suppose $\hat{\theta}(\ell) \in \mathbf{R}^{n_{\theta}}$ is an unbiased estimate of $\theta^{\text{true}} \in \mathbf{R}^{n_{\theta}}$. Under these conditions, the estimation error variance satisfies,

$$\mathbf{E} \|\hat{\theta}(\ell) - \theta^{\text{true}}\|^2 \geq V(\ell, \theta^{\text{true}}) = \text{Tr } G(\ell, \theta^{\text{true}})^{-1} \quad (103)$$

where

$$\begin{aligned} G(\ell, \theta^{\text{true}}) &= \sum_{\beta, \tau} \ell_{\beta\tau} G_{\beta\tau}(\theta^{\text{true}}) \in \mathbf{R}^{n_{\theta} \times n_{\theta}} \\ G_{\beta\tau}(\theta^{\text{true}}) &= \sum_{\alpha} \left(\frac{(\nabla_{\theta} p_{\alpha\beta\tau}(\theta)) (\nabla_{\theta} p_{\alpha\beta\tau}(\theta))^T}{p_{\alpha\beta\tau}(\theta)} - \nabla_{\theta\theta} p_{\alpha\beta\tau}(\theta) \right) \Big|_{\theta=\theta^{\text{true}}} \in \mathbf{R}^{n_{\theta} \times n_{\theta}} \end{aligned} \quad (104)$$

The relaxed experiment design problem with respect to the surrogate $\hat{\theta}$ for θ^{true} is,

$$\begin{aligned} &\text{minimize} \quad V(\lambda, \hat{\theta}) = \text{Tr} \left(\sum_{\beta, \tau} \lambda_{\beta\tau} G_{\beta\tau}(\hat{\theta}) \right)^{-1} \\ &\text{subject to} \quad \sum_{\beta, \tau} \lambda_{\beta\tau} = 1 \\ &\quad \lambda_{\beta\tau} \geq 0, \forall \beta, \tau \end{aligned} \quad (105)$$

with optimization variables $\lambda_{\beta\tau}$, the distribution of experiments per configuration $(\rho_{\beta}^{\text{init}}, t_{\tau})$. The difference between this and the previous formulation is that there are no equality constraints on the parameters. The gradient $\nabla_{\theta} p_{\alpha\beta\tau}(\theta)$ and Jacobian $\nabla_{\theta\theta} p_{\alpha\beta\tau}(\theta)$ are dependent on the parametric structure of the Hamiltonian $H(t, \theta)$.

4.3 Example: experiment design for Hamiltonian parameter estimation

Consider the system Hamiltonian,

$$H = \theta^{\text{true}} \varepsilon (X + Z) / \sqrt{2}, \quad (106)$$

with *constant* control ε . The goal is to select the control to make the Hadamard logic gate, $U_{\text{had}} = (X + Z) / \sqrt{2}$. If θ^{true} were known, then the control $\varepsilon = 1/\theta^{\text{true}}$ would produce the Hadamard (to within a scalar phase) at time $t = \pi/2$, that is,

$$U(t = \pi/2) = \exp \left\{ -i(\pi/2) H(\varepsilon = 1/\theta^{\text{true}}) \right\} = -i U_{\text{had}} \quad (107)$$

We assume that only the estimate $\hat{\theta}$ of θ^{true} is available. Using the estimate and knowledge of the Hamiltonian model structure, the control is $\varepsilon = 1/\hat{\theta}$. This yields the *actual* gate at $t = \pi/2$,

$$\begin{aligned} U_{\text{act}} &= \exp \left\{ -i(\pi/2) H(\varepsilon = 1/\hat{\theta}) \right\} = -i U_{\text{had}} \exp \left\{ -i\delta (\pi/2) U_{\text{had}} \right\} \\ \delta &= \theta^{\text{true}}/\hat{\theta} - 1 \end{aligned} \quad (108)$$

Since the parameter estimate, $\hat{\theta}$, is a random variable, so is the normalized parameter error δ . Assuming the estimate is unbiased, the expected value of the worst-case gate fidelity (1) is given explicitly by,

$$\mathbf{E} \min_{\|\psi\|=1} |(U_{\text{had}}\psi)^* (U_{\text{act}}\psi)|^2 = \mathbf{E} \cos^2 \left(\frac{\pi}{2} \delta \right) \approx 1 - \left(\frac{\pi}{2} \right)^2 \mathbf{E}(\delta^2) \quad (109)$$

Consider the case where the system is in the model set, the POVMs are projectors in the computational basis ($|0\rangle$, $|1\rangle$), and the configurations consist of combinations of input states and sample times. Specifically, the example problem is as follows:

$$\begin{aligned} \text{model Hamiltonian} \quad & H(\varepsilon, \theta) = \theta \varepsilon (X + Z) / \sqrt{2} \\ \text{true Hamiltonian} \quad & H^{\text{true}} = \theta^{\text{true}} \varepsilon (X + Z) / \sqrt{2} \\ \text{POVM} \quad & M_1 = |0\rangle\langle 0|, \quad M_2 = |1\rangle\langle 1| \\ \text{configurations} \quad & \left\{ \begin{array}{l} \text{sample times} \\ t_k = \delta(k-1), \quad k = 1, \dots, 100, \quad \delta = (\pi/2)/99 \\ \text{with pure input state} \\ \psi^{\text{init}} = |0\rangle \text{ or } \psi^{\text{init}} = U_{\text{had}}|0\rangle \end{array} \right. \end{aligned} \quad (110)$$

In this example, with a single parameter and a single input state, the optimal experiment design problem (105) becomes:

$$\begin{aligned} \text{minimize} \quad & V(\lambda, \theta^{\text{surr}}) = (\sum_{\tau} \lambda_{\tau} g_{\tau}(\theta^{\text{surr}}))^{-1} \\ \text{subject to} \quad & \sum_{\tau} \lambda_{\tau} = 1 \\ & \lambda_{\tau} \geq 0, \quad \forall \tau \end{aligned} \quad (111)$$

The trace operation in (105) is eliminated because the matrix $G_{\beta\tau}(\theta^{\text{surr}})$ is now the scalar,

$$g_{\tau}(\theta^{\text{surr}}) = \sum_{\alpha} \left(\frac{(\nabla_{\theta} p_{\alpha\tau}(\theta)) (\nabla_{\theta} p_{\alpha\tau}(\theta))^T}{p_{\alpha\tau}(\theta)} - \nabla_{\theta\theta} p_{\alpha\tau}(\theta) \right) \Big|_{\theta=\theta^{\text{surr}}} \in \mathbf{R} \quad (112)$$

The solution can be determined directly: concentrate all the experiments at the recording time t_{τ} where $g_{\tau}(\theta^{\text{surr}})$ is a maximum, specifically,

$$t^{\text{opt}} = \{ t_s \mid g_s(\theta^{\text{surr}}) \geq g_{\tau}(\theta^{\text{surr}}), \quad \forall s, \tau \} \quad (113)$$

The following tables show the minimum number of experiments at the optimal recording time, t^{opt} , in order to achieve 0.01 accuracy (deviation) in the parameter estimate with $\theta^{\text{surr}} = \theta^{\text{true}}$. The two cases shown are for the two input states with the control set to unity.

$$\begin{array}{c} \varepsilon = 1 \\ \psi^{\text{init}} = |0\rangle \end{array} \quad \begin{array}{c} \varepsilon = 1 \\ \psi^{\text{init}} = U_{\text{had}}|0\rangle \end{array}$$

$\theta^{\text{surr}} = \theta^{\text{true}}$	$t^{\text{opt}}/(\pi/2)$	ℓ_{expt}
0.9	0.68	8,876
1.0	0.61	10,957
1.1	0.56	13,262

$\theta^{\text{surr}} = \theta^{\text{true}}$	$t^{\text{opt}}/(\pi/2)$	ℓ_{expt}
0.9	1.0	2052
1.0	1.0	2069
1.1	1.0	2052

(114)

To make the Hadamard the control update is $\varepsilon = 1/\hat{\theta}$ which follows from the (risky) assumption that the estimate, $\hat{\theta}$, is perfectly correct. For any of the true values from the above table (114), all the estimates have the same accuracy. Hence, the average value of the worst-case gate fidelity after the update is approximately,

$$\mathbf{E} \min_{\|\psi\|=1} |(U_{\text{des}}\psi)^* (U_{\text{act}}\psi)|^2 \approx 1 - \left(\frac{\pi}{2}\right)^2 (0.01^2) = 1 - 0.00024672 = 0.999753 \quad (115)$$

The ease of obtaining the estimate by minimizing the negative log-likelihood function can be determined by examining the *average likelihood function*,

$$\mathbf{E} L(\theta) = \sum_{\alpha, \gamma} \ell_{\gamma} p_{\alpha\gamma}(\theta^{\text{true}}) \log p_{\alpha\gamma}(\theta) \quad (116)$$

which is obtained from (102) and (6). Figure 8 shows plots of normalized⁹ $\mathbf{E} L(\theta)$, $0.8 \leq \theta \leq 1.2$ for the three true parameter values and corresponding optimal recording times from the table in (114) with control $\varepsilon = 1$ and initial state $|0\rangle$. In all three cases, over the θ range shown, $\mathbf{E} L(\theta)$ is convex.

Figure 9 shows plots of normalized $\mathbf{E} L(\theta)$, $0.8 \leq \theta \leq 1.2$ for the three true parameter values and corresponding optimal recording times from the table in (114) with control $\varepsilon = 1$ and initial state $U_{\text{had}}|0\rangle$. For initial state $|0\rangle$, a range of 8876 to 13262 experiments are needed at the optimal recording time to achieve 0.01 deviation in the estimate. With the initial states $U_{\text{had}}|0\rangle$ the same accuracy only requires about 2000 experiments. This difference can be inferred partly by comparing the curvature in the plots in Figure 8 with 9; as they are plotted on the same normalized scale. Note the increased curvature of $\mathbf{E} L(\theta)$ in Figure 9 in the neighborhood of the true value.

If we further increase the control effort, say to $\varepsilon = 5$, the number of experiments required to achieve 0.01 accuracy is significantly reduced as seen in the following table.

$$\begin{array}{c} \varepsilon = 5 \\ \psi^{\text{init}} = |0\rangle \end{array}$$

$\theta^{\text{surr}} = \theta^{\text{true}}$	$t^{\text{opt}}/(\pi/2)$	ℓ_{expt}
0.9	0.93	98
1.0	0.84	121
1.1	1.00	122

(117)

⁹The plots show $\mathbf{E} L(\theta)$ divided by its minimum value, thus *normalized* to have a minimum of unity.

However, Figure 10 shows clearly that the average likelihood function is now significantly more oscillatory, and certainly not convex over the range shown. It is of course convex in a much smaller neighborhood of the true value. This would require, therefore, very precise prior knowledge about the true system. Thus we see a clear tradeoff between the number of experiments to achieve a desired estimation accuracy and the ease of obtaining the estimate as seen by the convexity, or lack thereof, with respect to minimizing the likelihood function, which is the optimization objective.

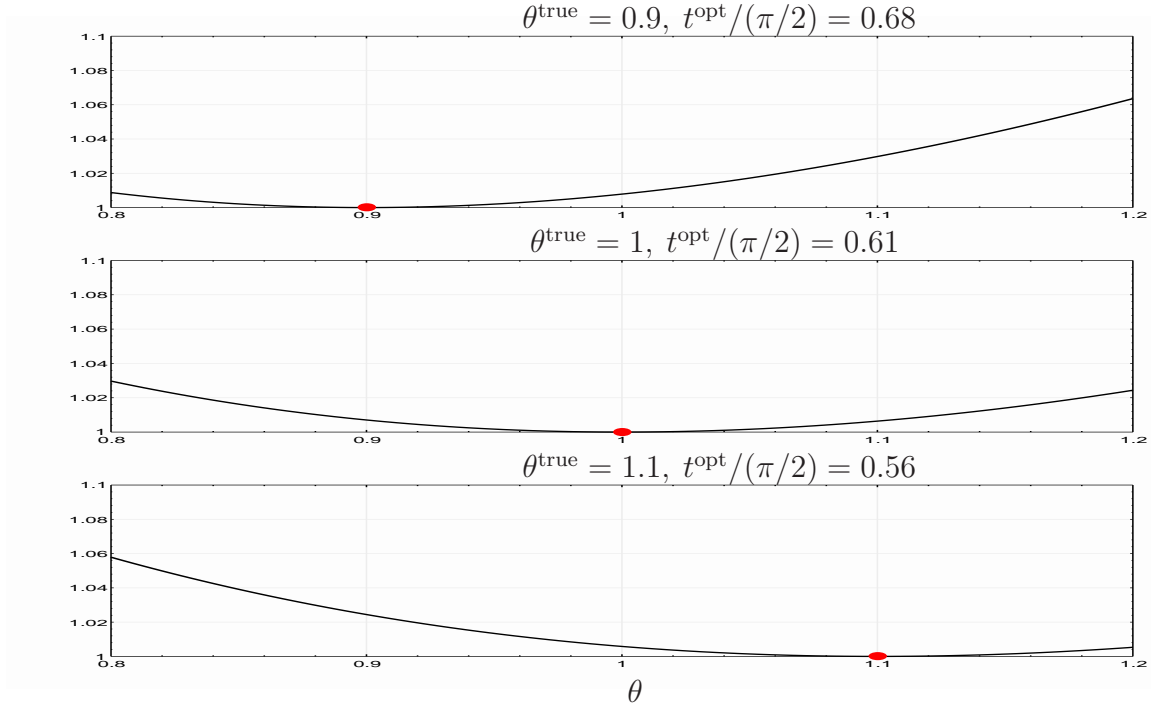


Figure 8: Normalized average likelihood function $E L(\theta)$ with control $\varepsilon = 1$ and input state $\psi^{\text{init}} = |0\rangle$ for the true parameter values and associated optimal recording times as indicated above and given in (114).

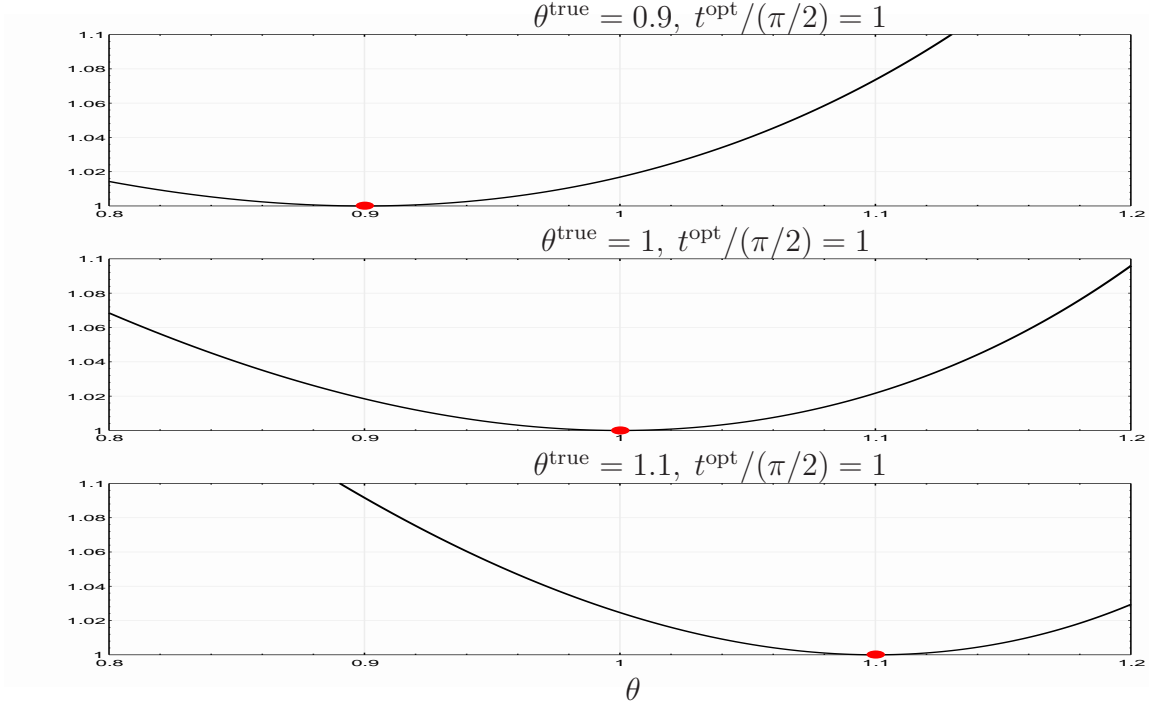


Figure 9: Normalized average likelihood function $\mathbf{E} L(\theta)$ with control $\varepsilon = 1$ and initial state $\psi^{\text{init}} = U_{\text{had}}|0\rangle$ for the true parameter values and associated optimal recording times as indicated above and given in (114).

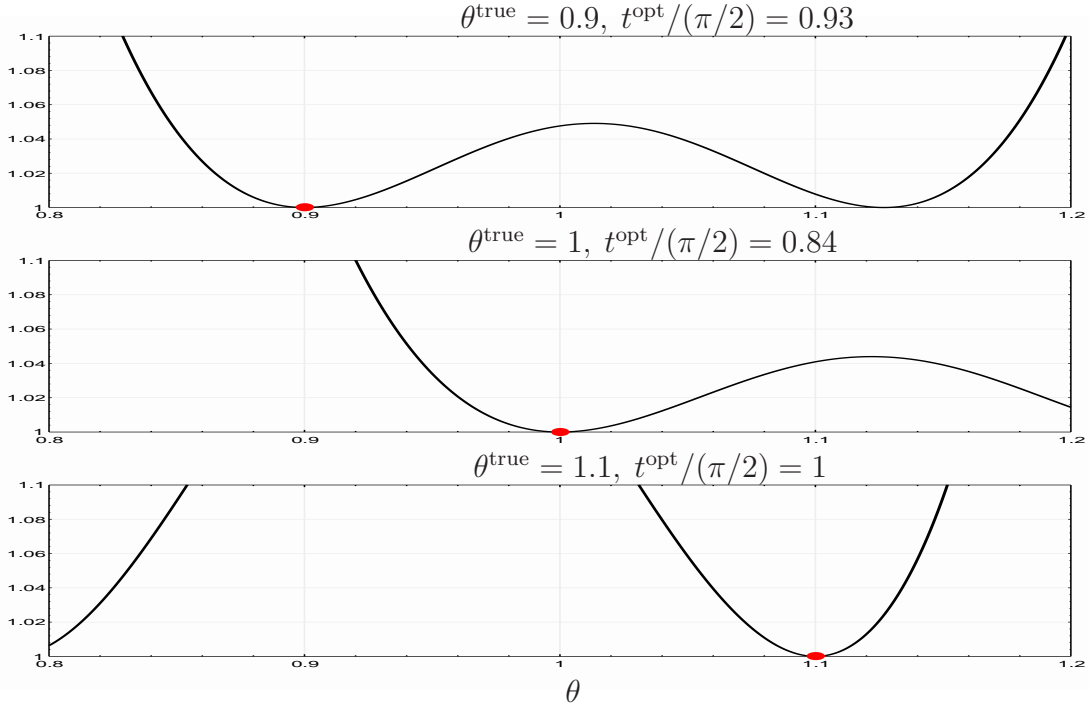


Figure 10: Normalized average likelihood function $\mathbf{E} L(\theta)$ with control $\varepsilon = 5$ and initial state $\psi^{\text{init}} = |0\rangle$ for the true parameter values and associated optimal recording times as indicated above and given in (117).

5 Summarizing Maximum Likelihood Estimation & Optimal Experiment Design

The results presented show that an efficient numerical method based on convex programming is possible for optimizing the experiment for state and process tomography. In addition, the estimation of the state and/or process using data from non-continuing measurements is copacetic with Maximum Likelihood Estimation. Both the experiment design and estimation work naturally together and both can be solved using convex optimization methods.

Maximum likelihood estimation

The general form for estimating the parameter π^{true} is obtained as the solution to the optimization problem,

$$\begin{array}{ll} \text{minimize} & L(\pi) = -\sum_{\alpha,\gamma} n_{\alpha\gamma} \log p_{\alpha\gamma}(\pi) \\ \text{subject to} & \pi \in \Pi \end{array} \quad (118)$$

Under the assumption that the system generating the data is in the model set used for estimation, the estimate, π^{ML} , the solution to (118), is unbiased and has the asymptotic variance,

$$\mathbf{E} \|\pi^{\text{ML}} - \pi^{\text{true}}\|^2 \rightarrow \frac{1}{\ell_{\text{expt}}} V(\lambda, \pi^{\text{true}}) \quad \text{as } \ell_{\text{expt}} \rightarrow \infty \quad (119)$$

where λ is the vector of fraction of experiments per configuration, and $V(\lambda, \pi^{\text{true}})$ is obtained from the Cramér-Rao inequality.

Optimal experiment design

The general form for estimating the configuration distribution λ is obtained as the solution to the optimization problem,

$$\begin{array}{ll} \text{minimize} & V(\lambda, \hat{\pi}) = \text{Tr} \left(\sum_{\gamma} \lambda_{\gamma} G_{\gamma}(\hat{\pi}) \right)^{-1} \\ \text{subject to} & \sum_{\gamma} \lambda_{\gamma} = 1, \quad \lambda_{\gamma} \geq 0 \end{array} \quad (120)$$

where $\hat{\pi}$ is a surrogate for π^{true} .

Tables 1 and 2 summarize the class of estimation and experiment design problems, respectively.

objective	$p_{\alpha\gamma}(\pi)$	$\pi \in \Pi$	comment
Hamiltonian parameter estimation	$p_{\alpha\gamma}(\theta) = \text{Tr } O_{\alpha\gamma}(\theta) \rho_\gamma$	$\ \theta - \theta_{\text{nom}}\ \leq \delta$	not convex in θ many local minima
state estimation	$p_{\alpha\gamma}(\rho) = \text{Tr } O_{\alpha\gamma} \rho$	$\text{Tr } \rho = 1, \rho \geq 0$	convex in ρ
state distribution estimation	$p_{\alpha\gamma}(f) = a_{\alpha\gamma}^T f$ $(a_{\alpha\gamma})_i = \text{Tr } O_{\alpha\gamma} \rho_i$	$\sum_i f_i = 1, f_i \geq 0$	convex in f
OSR fixed basis (B_i)	$p_{\alpha\gamma}(X) = \text{Tr } R_{\alpha\gamma} X$ $[R_{\alpha\gamma}]_{ij} = \text{Tr } B_j^* M_{\alpha\gamma} B_i \rho_\gamma$	$X \geq 0$ $\sum_{i,j} X_{ij} B_i^* B_j = I$	convex in X
OSR distribution (\bar{K}_i basis)	$p_{\alpha\gamma}(q) = a_{\alpha\gamma}^T q$ $(a_{\alpha\gamma})_i = \text{Tr } M_{\alpha\gamma} \bar{K}_i \rho_\gamma \bar{K}_i^*$	$\sum_i q_i = 1, q_i \geq 0$	convex in q

Table 1: Summary of maximum likelihood estimation. Except for Hamiltonian parameter estimation, all other cases are convex optimization problems.

objective	$p_{\alpha\gamma}(\pi^{\text{surr}})$	$G_\gamma(\pi^{\text{surr}})$
Hamiltonian parameter estimation	$p_{\alpha\gamma}(\theta^{\text{surr}}) = \text{Tr } O_{\alpha\gamma}(\theta^{\text{surr}}) \rho_\gamma$	$\sum_\alpha \left(\frac{1}{p_{\alpha\gamma}} (\nabla_\theta p_{\alpha\gamma}) (\nabla_\theta p_{\alpha\gamma})^T - \nabla_{\theta\theta} p_{\alpha\gamma} \right)$
state estimation	$p_{\alpha\gamma}(\rho^{\text{surr}}) = \text{Tr } O_{\alpha\gamma} \rho^{\text{surr}}$	$C_{\text{eq}}^* \left(\sum_\alpha \frac{1}{p_{\alpha\gamma}} (\text{vec } O_{\alpha\gamma}) (\text{vec } O_{\alpha\gamma})^* \right) C_{\text{eq}}$
state distribution estimation	$p_{\alpha\gamma}(f^{\text{surr}}) = a_{\alpha\gamma}^T f^{\text{surr}}$ $(a_{\alpha\gamma})_i = \text{Tr } O_{\alpha\gamma} \rho_i$	$C_{\text{eq}}^* \left(\sum_\alpha \frac{1}{p_{\alpha\gamma}} a_{\alpha\gamma} a_{\alpha\gamma}^T \right) C_{\text{eq}}$
OSR fixed basis (B_i)	$p_{\alpha\gamma}(X^{\text{surr}}) = \text{Tr } R_{\alpha\gamma} X^{\text{surr}}$ $[R_{\alpha\gamma}]_{ij} = \text{Tr } B_j^* M_{\alpha\gamma} B_i \rho_\gamma$	$C_{\text{eq}}^* \left(\sum_\alpha \frac{1}{p_{\alpha\gamma}} (\text{vec } R_{\alpha\gamma}) (\text{vec } R_{\alpha\gamma})^* \right) C_{\text{eq}}$
OSR distribution (\bar{K}_i basis)	$p_{\alpha\gamma}(q^{\text{surr}}) = a_{\alpha\gamma}^T q^{\text{surr}}$ $(a_{\alpha\gamma})_i = \text{Tr } M_{\alpha\gamma} \bar{K}_i \rho_\gamma \bar{K}_i^*$	$C_{\text{eq}}^* \left(\sum_\alpha \frac{1}{p_{\alpha\gamma}} a_{\alpha\gamma} a_{\alpha\gamma}^T \right) C_{\text{eq}}$

Table 2: Summary of optimal experiment designs. These are convex optimization problems in all cases. The matrix C_{eq} comes from the associated parameter equality constraints, *e.g.*, $\text{Tr } \rho^{\text{surr}} = 1$, $\sum_i f_i^{\text{surr}} = 1$, $\sum_{i,j} X_{ij}^{\text{surr}} B_i^* B_j = I$, *etc.*

6 Iterative Adaptive Control

Quantum process tomography can be used for adaptive control design as described in [20]. Adaptive control systems are in general one of two types [2, 1]: (1) *indirect adaptive control* – use the data to first determine parameters in a system model, then based on the model determine the control parameters, and (2) *direct adaptive control* – use the data to directly select control parameters by comparing actual performance to an ideal. Applications of direct adaptive control (and learning principles) to quantum systems can be found in [30, 41, 31]. It could be argued that the direct approach is simpler in that a system model is not needed. However, this is a little deceptive because in effect the *closed-loop system* is being modeled indirectly via the ideal performance. This is made more explicit in the *unfalsification/invalidation* approach to adaptive control, [34], [19].

6.1 Indirect adaptive control

Hamiltonian parameter estimation and associated optimal experiment design can be combined in an iterative indirect adaptive control approach as depicted in Figure 11.

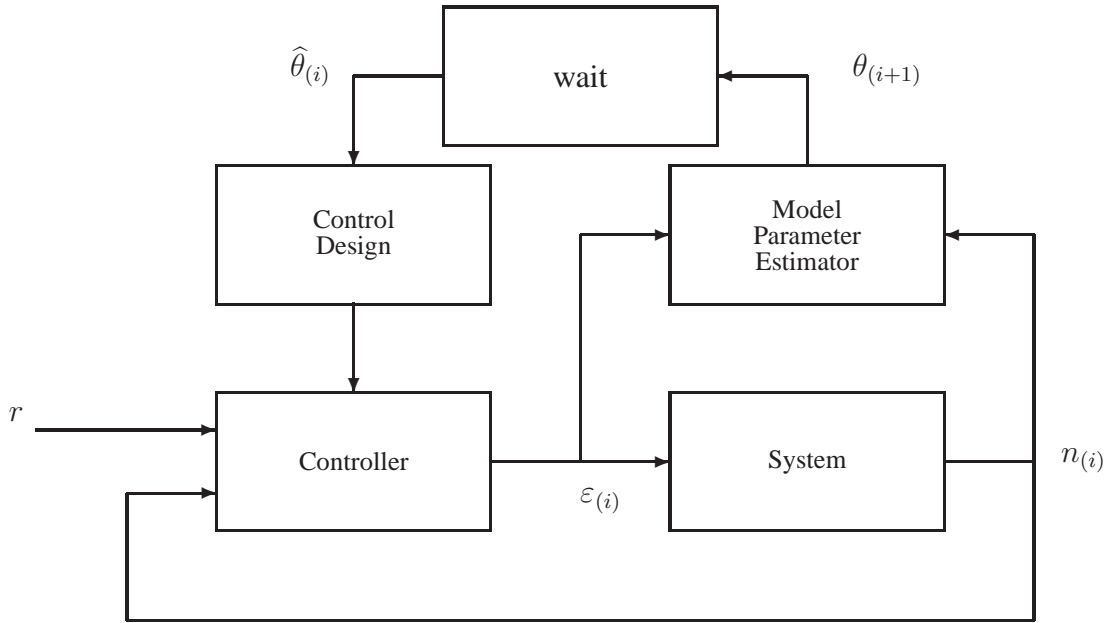


Figure 11: Iterative adaptive control

Typical steps in the iteration are:

$$\begin{aligned}
\text{control design} \quad & \varepsilon^{(i)} = \arg \text{opt}_{\varepsilon} J(\varepsilon, \theta^{(i)}) \\
\text{experiment design} \quad & \ell^{(i)} = \mathbf{round}(\ell_{\text{expt}} \lambda^{(i)}) \\
& \lambda^{(i)} = \arg \min \left\{ V(\lambda, \varepsilon^{(i)}, \theta^{(i)}) \mid \lambda \geq 0, \sum_{\gamma} \lambda_{\gamma} = 1 \right\} \\
\text{collect data} \quad & D^{(i)} = \left\{ n_{\alpha\gamma}^{(i)} \mid \alpha = 1, \dots, n_{\text{out}}, \gamma = 1, \dots, n_{\text{cfg}} \right\} \\
\text{estimate parameters} \quad & \theta^{(i+1)} = \arg \min \left\{ L(D^{(i)}, \theta) \mid \|\theta - \theta_{\text{nom}}\| \leq \delta \right\}
\end{aligned} \tag{121}$$

The “opt” in the control design step could be to maximize worst-case gate fidelity (1),

$$\varepsilon^{(i)} = \max_{\varepsilon} \underbrace{\min_{\|\psi\|=1} \left| (U_{\text{des}}\psi)^* (U(t_f, \varepsilon, \theta^{(i)})\psi) \right|^2}_{J(\varepsilon, \theta^{(i)})} \tag{122}$$

where $U(t, \varepsilon, \theta)$ is the propagator arising from the parametric Hamiltonian model. The control design step is not necessarily convex. Even if it were, it is not yet known under what conditions the complete iterative procedure will converge to the optimal control, or converge at all [20]. For example, in the simulations to follow convergence to the optimum is dependent on the initial parametrization. The properties of this type of iteration remain an area for further study.

Example

The spin-coherent photon transmitter/receiver system proposed in [38, 40] creates quantum logic gates by manipulating electron spin via external potentials (gate voltages) to effect the *g-factors* in the semiconductor material in the presence of an external (rotating) magnetic field ([18] explores *g-tensor* control without the rotating field). Following [11, III, Ch.12-9] on models of spin systems, an idealized model of the normalized Hamiltonian in the rotating frame of a two-qubit gate under “linear g-factor control” is given by,

$$\begin{aligned}
H &= H_1 + H_2 + H_{12} \\
H_1 &= \frac{1}{2} [\varepsilon_{1z}\omega_0(Z \otimes I_2) + \varepsilon_{1x}\omega_1(X \otimes I_2)] \\
H_2 &= \frac{1}{2} [\varepsilon_{2z}\omega_0(I_2 \otimes Z) + \varepsilon_{2x}\omega_1(I_2 \otimes X)] \\
H_{12} &= \varepsilon_c\omega_c (X^{\otimes 2} + Y^{\otimes 2} + Z^{\otimes 2})
\end{aligned}$$

The design goal is to use the 5 controls ($\varepsilon_{1z}, \varepsilon_{1x}, \varepsilon_{2z}, \varepsilon_{2x}, \varepsilon_c$) to make the Bell transform,

$$U_{\text{bell}} = \frac{1}{\sqrt{2}} \begin{bmatrix} 1 & 0 & 1 & 0 \\ 0 & 1 & 0 & 1 \\ 0 & 1 & 0 & -1 \\ 1 & 0 & -1 & 0 \end{bmatrix}$$

One of the many possible decompositions of the Bell transform is the following:

$$U_{\text{bell}} = (U_{\text{had}} \otimes I_2) \sqrt{U_{\text{swap}}} (X^{-1/2} \otimes X^{1/2}) \sqrt{U_{\text{swap}}} (I_2 \otimes X)$$

Each operation in this sequence uses only the single qubit and swap “gates” produced by simultaneously pulsing the 5 controls as shown in the following table.

ε_{1z}	ε_{1x}	ε_{2z}	ε_{2x}	ε_c	Δt	gate
0	0	0	1	0	$\frac{\pi}{\omega_1}$	$-iI_2 \otimes X$
0	0	0	0	1	$\frac{\pi}{8\omega_c}$	$e^{-i\frac{\pi}{8}} \sqrt{U_{\text{swap}}}$
0	0	0	1	0	$\frac{\pi}{2\omega_1}$	$e^{-i\frac{\pi}{4}} I_2 \otimes X^{1/2}$
0	1	0	0	0	$\frac{3\pi}{2\omega_1}$	$e^{-i\frac{3\pi}{4}} X^{-1/2} \otimes I_2$
0	0	0	0	1	$\frac{\pi}{8\omega_c}$	$e^{-i\frac{\pi}{8}} \sqrt{U_{\text{swap}}}$
$\frac{\omega_{\text{had}}}{\omega_0\sqrt{2}}$	$\frac{\omega_{\text{had}}}{\omega_1\sqrt{2}}$	0	0	0	$\frac{\pi}{\omega_{\text{had}}}$	$-iU_{\text{had}} \otimes I_2$

Figure 12: Pulse control table

The resulting gate at the final time, t_f , is U_{bell} to within a scalar phase:

$$U(t_f) = e^{-i\frac{\pi}{4}} U_{\text{bell}}, \quad t_f = \left(\frac{3}{\omega_1} + \frac{1}{4\omega_c} + \frac{1}{\omega_{\text{had}}} \right) \pi$$

Suppose the only unknown parameter is ω_1 . Consider the following simplified version of (121):

$$\begin{aligned} \text{control design} \quad & \varepsilon^{(i)} = \bar{\varepsilon}(\hat{\omega}_1^{(i)}), \quad t_f^{(i)} = t_f(\hat{\omega}_1^{(i)}) \\ \text{estimation} \quad & \hat{\omega}_1^{(i+1)} = \arg \min_{\omega_1} \mathbf{E} L(\omega_1, \varepsilon^{(i)}) \end{aligned}$$

where the control design function $\bar{\varepsilon}(\hat{\omega}_1^{(i)})$ represents the pulse design from the above table, and where the average likelihood function follows from the description in Section §4.1 with the following parameters:

$$\begin{aligned} \text{single initial state} \quad & \rho^{\text{init}} = |0\rangle\langle 0| \quad (\beta = 1) \\ \text{POVM} \quad & M_1 = |0\rangle\langle 0|, \quad M_2 = |1\rangle\langle 1| \quad (n_{\text{out}} = 2) \\ \text{sample times} \quad & \text{either } \{t_f(\hat{\omega}_1), (n_{\text{sa}} = 1)\} \text{ or } \{t_f(\hat{\omega}_1)/2, t_f(\hat{\omega}_1), (n_{\text{sa}} = 2)\} \end{aligned}$$

Using Hamiltonian parameters ($\omega_0^{\text{true}} = 1$, $\omega_1^{\text{true}} = 0.01$, $\omega_c^{\text{true}} = 0.01$), Figure 13 shows $\mathbf{E} L(\hat{\omega}_1, n_{\text{sa}} = 1)$ vs. $\hat{\omega}_1/\omega_1^{\text{true}}$ for sequences of adaptive iterations using the estimate $\hat{\omega}_1$ obtained from a local hill climbing algorithm, *i.e.*, the local maximum of the average likelihood

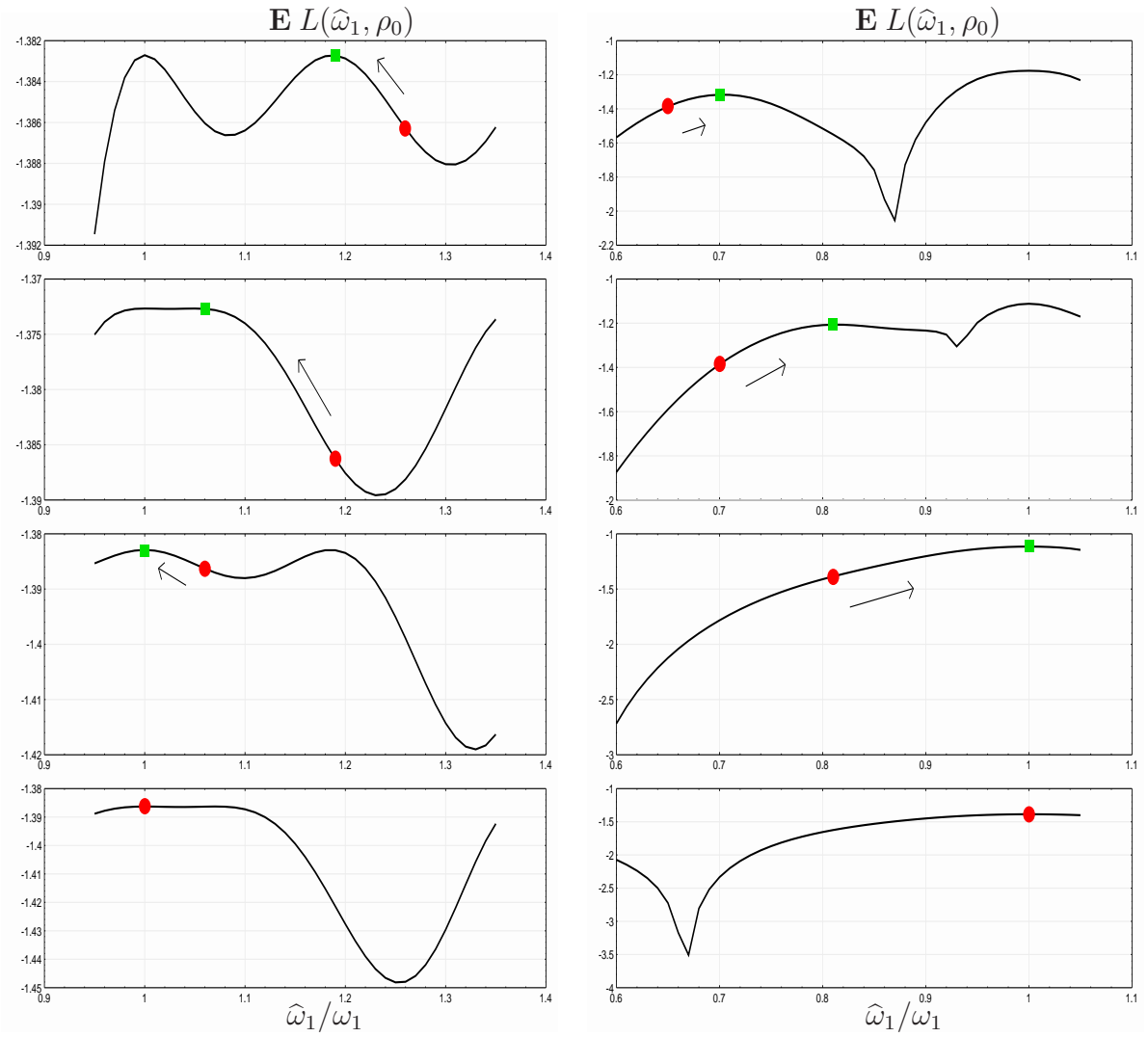


Figure 13: Iterative adaptation for $n_{sa} = 1$ at $t_f(\hat{w}_1)$ for two starting values of \hat{w}_1 .

function is obtained. The estimation is followed by a control using the estimated value in the pulse control table. In the two cases shown the algorithm converges to the true value.

Although not shown, the algorithm does not converge from all initial values of \hat{w}_1 . Figure 14 shows $\|U(t_f(\hat{w}_1), \bar{\varepsilon}(\hat{w}_1)) - U_{des}\|_{frob}$ vs. estimate $\hat{w}_1/\omega_1^{true}$ with the control from the table. The function is clearly not convex. The region of convergence for $n_{sa} = 1$ and $n_{sa} = 2$ sample times are shown in blue and green, respectively. The region of attraction is increased for $n_{sa} = 2$. These results, of course, are specific to this example and can not be generalized. To re-iterate, conditions for convergence, region of attraction, and so on, are only partially understood, in general, for this type of iteration [16].

6.2 Direct adaptive control

In a direct adaptive control system no model is posed for the system; ideally only a performance measure is available and the control parameters are adjusted to improve the performance. The

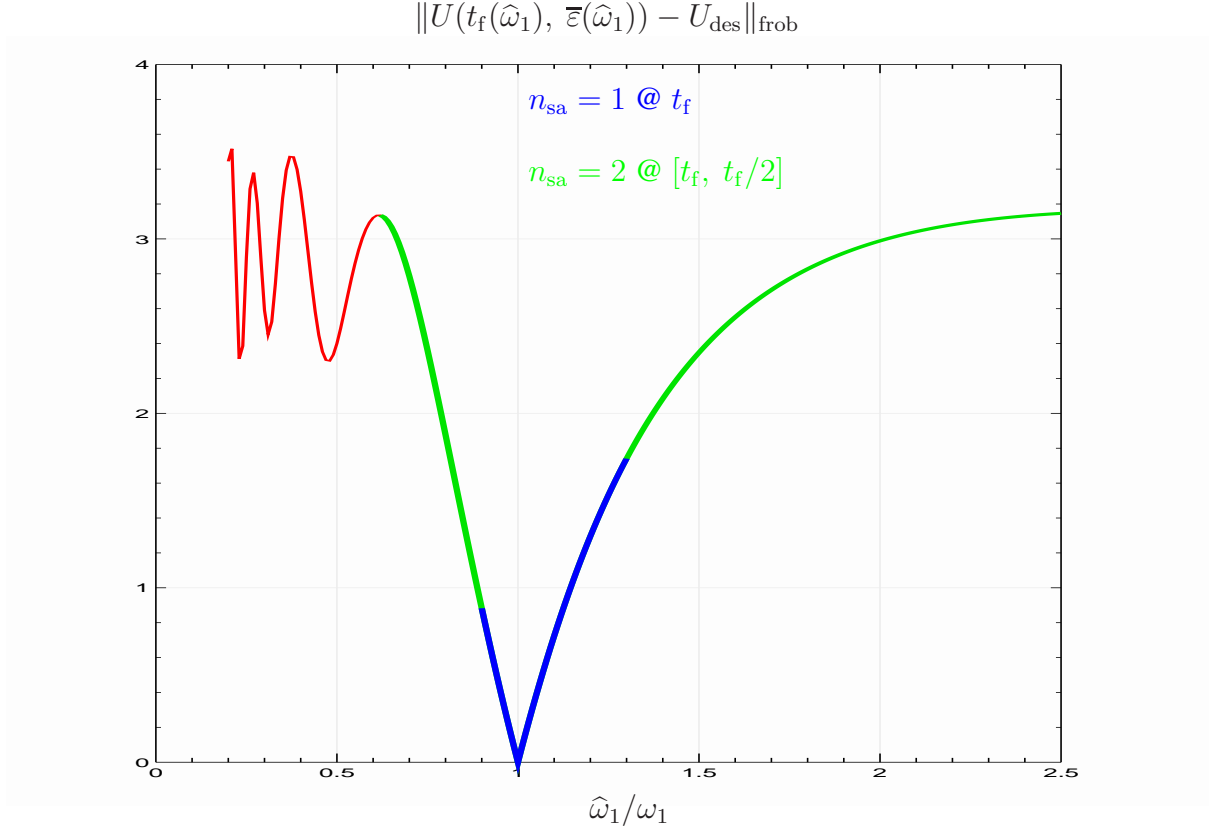


Figure 14: Regions of convergence.

adjustment “directions”, however, clearly must depend on the shape of the “landscape”, otherwise, it would not be possible to know how to make the adjustment. In effect then, a model of the landscape is either available or is computed intrinsically. Consider the following bipartite system whose Hamiltonian depends on the two controls $(\varepsilon_z, \varepsilon_x)$.

$$\begin{aligned}
 H(\varepsilon) &= H_Q(\varepsilon) \otimes I_E + I_Q \otimes H_E + H_{QE} \\
 H_Q(\varepsilon) &= (\varepsilon_z - 1)\omega_{Qz}Z/2 + \varepsilon_x\omega_{Qx}X/2 \\
 H_E &= \omega_{Ez}Z/2 + \omega_{Ex}X/2 \\
 H_{QE} &= \omega_{QE}(X^{\otimes 2} + Y^{\otimes 2} + Z^{\otimes 2})
 \end{aligned}$$

The Q-part of the system is assumed to be accessible to the user and the E-part, the “environment”, is not. The goal is to select the controls to make the Q-system behave as a *bit-flip* device, *i.e.*, the Pauli X matrix. Suppose the Q-system is prepared in the initial state $\rho_Q^{\text{init}} = |1\rangle\langle 1|$ and a measurement is made at $t_f = \pi/\omega_{Qx}$ of the state $|0\rangle$. hence, ideally, the outcome probability, $p(\varepsilon)$, should be unity. Due to the uncontrolled E -system coupling, however, the goal is to select the controls ε to make $p(\varepsilon)$ as large as possible. Under these conditions the outcome probability $p(\varepsilon)$ arises from,

$$\begin{aligned}
 p(\varepsilon) &= \text{Tr } MU(t_f)\rho_0U(t_f)^* \\
 i\dot{U}(t) &= H(\varepsilon(t))U(t), \quad U(0) = I, \quad 0 \leq t \leq t_f \\
 \rho_0 &= \rho_Q^{\text{init}} \otimes \rho_E^{\text{init}}
 \end{aligned}$$

Of course the system Hamiltonian is not known, only at best the outcome probability would be known after enough repetitions of the experiment.

Figure 15 shows the landscape of the system with parameters, $\omega_{Qz} = 1$, $\omega_{Qx} = 0.01$, $\omega_{Ez} = 1$, $\omega_{Qx} = 0$, $\omega_{QE} = 0.005$, $\rho_E^{\text{init}} = I_2/2$ and for *constant* values of the controls over the ranges $0.96 \leq \varepsilon_z \leq 1.04$, $0.1 \leq \varepsilon_x \leq 5.2$.

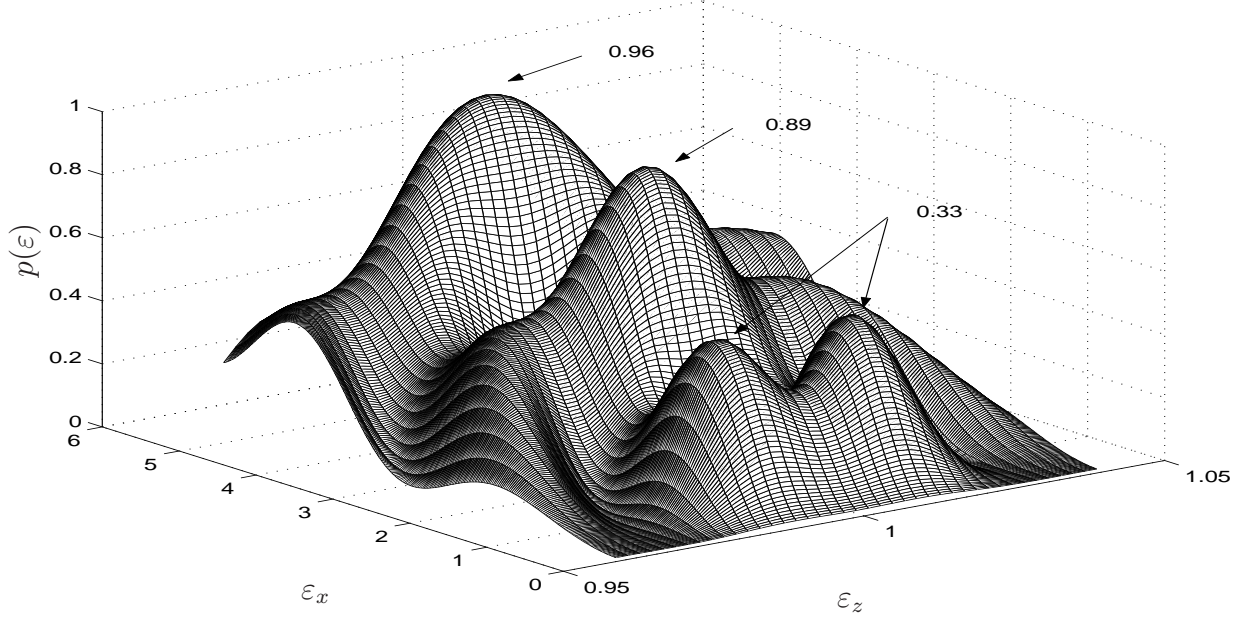


Figure 15: Two parameter landscape; the maximum probability of 0.96 is achieved with $\varepsilon_z = 0$ and $\varepsilon_x = 5.2$.

The landscape clearly has several local maximum values. Thus without some knowledge of the landscape or an exhaustive search, it might be difficult to find the global maximum. In this two-parameter case, of course, an exhaustive search is not too exhausting. Nevertheless, it is clear that any direct adaptive algorithm will face some difficulties. It is also clear that prior knowledge can alleviate many of the difficulties, *e.g.*, knowledge of system parameter ranges or nominal response which is close to a good outcome, *etc.*

A more in-depth analysis of the landscape for control of quantum systems can be found in [32]. There it is shown that for unconstrained time-varying controls, if the system is controllable, then *all* the local maximum are global. That is, the outcome probability at every local maximum is unity and all other extrema give the minimum probability of zero. The complexity shown here results principally from the fact that the choice of controls is constrained to be constant. This points out the importance of constraints either imposed by the physics or by the designer in inadvertently making the "wrong" choice of the control structure. In particular, suppose that the landscape is actually very simple with even possibly one extremum when viewed with no constraints on the controls. However, when constraints are imposed, or a new set of controls is defined, the landscape may then exhibit structure that was not evident in the freely floating original set. An extreme opposite case could be for a choice of variables where the new variables actually do hardly anything at all with regard to control action. In this case one would conclude that the landscape is totally flat!

Many of the current "working" adaptive feedback control experiments are operating some-

where between these two extremes, ranging from having highly constrained knobs to the totally wrong knobs. This comment comes from the observation that physical effects spanning a dynamic range in quantum wavelength of about 10^7 are being controlled by a single type of laser, *i.e.*, the Ti:Sapphire laser, working over a range of about 1-10 on that scale. That is, a domain in laser wavelength of 10 (in some units) is split up into about 100 small pieces as controls, and those very narrow controls manage everything over a huge dynamic range. The fact that the experiments work at all is rather amazing. A guess is that an examination of the landscapes will show considerable detail, much of which is likely false structures arising from having highly constrained controls. From a positive perspective, as more bandwidth becomes available the control landscape will become less complicated and more regular in the sense that more of the local optimum values will provide performance close to the global optimum.

A Appendix

A.1 Worst-case gate fidelity

From the definition of worst-case fidelity (1),

$$\begin{aligned} |(U_{\text{des}}\psi)^* (U_{\text{act}}\psi)|^2 &= |\psi^* (U_{\text{des}}^* U_{\text{act}}) \psi|^2 \\ &= |(V^* \psi)^* \Omega (V^* \psi)|^2 \\ &= \left| \sum_{k=1}^n \omega_k |x_k|^2 \right|^2 \\ &= \left| \sum_{k=1}^n \omega_k z_k \right|^2 \end{aligned}$$

where the last three lines follow directly from (i) the eigenvalue decomposition of the unitary: $U_{\text{des}}^* U_{\text{act}} = V \Omega V^*$, $V^* V = I_n$, $\Omega = \text{diag}(\omega_1 \cdots \omega_n)$, $|\omega_k| = 1$, (ii) defining $x = V^* \psi \in \mathbf{C}^n$, and (iii) defining $z_k = |x_k|^2 \in \mathbf{R}$. Using the definitions of the vectors (a, b) in (2) gives,

$$|(U_{\text{des}}\psi)^* (U_{\text{act}}\psi)|^2 = \left| \sum_{k=1}^n (a_k + ib_k) z_k \right|^2 = z^T (aa^T + bb^T) z$$

The QP follows from the relations:

$$\|\psi\| = 1 \Leftrightarrow \|x = V^* \psi\| = 1 \Leftrightarrow \sum_k (z_k = |x_k|^2) = 1, z_k \geq 0$$

A.2 Cramér-Rao Inequality

The following is the classical form of the Cramér-Rao Inequality.

Cramér-Rao Inequality[8]

Let $\theta_0 \in \mathbf{R}^p$ be the true parameter to be estimated from a data set D . Let $L(D, \theta_0)$ be the true negative log-likelihood function of the system generating the data. Let $\hat{\theta} \in \mathbf{R}^p$ be an unbiased estimate of θ_0 , *i.e.*, $\mathbf{E} \hat{\theta} = \theta_0$. Then, the covariance of the estimate,

$$\text{cov} \hat{\theta} = \mathbf{E} (\hat{\theta} - \theta_0) (\hat{\theta} - \theta_0)^T \quad (123)$$

satisfies the matrix inequality,

$$\begin{bmatrix} \text{cov } \hat{\theta} & I \\ I & F(\theta_0) \end{bmatrix} \geq 0 \quad (124)$$

where $F(\theta_0)$ is the *Fisher information matrix*,

$$F(\theta_0) = \mathbf{E} \nabla_{\theta\theta} L(D, \theta) \Big|_{\theta=\theta_0} \quad (125)$$

If $F(\theta_0) > 0$, then (124) is equivalent to,

$$\text{cov } \hat{\theta} \geq F(\theta_0)^{-1} \quad (126)$$

This famous theorem states the for any unbiased estimator, the covariance of the estimate satisfies the inequality (124), or equivalently (126), provided the Fisher matrix is invertible. Usually only (126) is given as the theorem: the minimum covariance of the estimate is given by the inverse of the Fisher information matrix. The power of the result (124) is that it is independent of *how* the estimate is obtained. The lower bound only depends on the model structure, the experiment design, and the information in the data.

A.3 Derivation of (28)

Define the vectors $r, a_{\alpha\gamma} \in \mathbf{C}^{n^2}$ as,

$$r = \text{vec } \rho, \quad a_{\alpha\gamma} = \text{vec } O_{\alpha\gamma}$$

Then

$$p_{\alpha\gamma} = \text{Tr } O_{\alpha\gamma} \rho = a_{\alpha\gamma}^* r$$

and

$$\text{Tr } \rho = 1 \Leftrightarrow b^T r = 1, \quad b = \text{vec } I_n$$

The next step eliminates the equality constraint $b^T r = 1$ reducing the n^2 unknowns in r to $n^2 - 1$. Since $b^T b = n$, the SVD of b is,

$$b = W \begin{bmatrix} \sqrt{n} \\ 0_{n^2-n} \end{bmatrix}$$

with unitary $W \in \mathbf{R}^{n^2 \times n^2}$, Partition $W = [c \ C_{\text{eq}}]$ with $C_{\text{eq}} \in \mathbf{R}^{n^2 \times n^2-1}$. Then all r satisfying $b^T r = 1$ are given by

$$r = c/\sqrt{n} + C_{\text{eq}} z$$

for all $z \in \mathbf{C}^{n^2-1}$. The likelihood function with the equality constraint ($\text{Tr } \rho = 1$ or $b^T r = 1$) eliminated is then a function only of z ,

$$L(D, z) = - \sum_{\alpha, \gamma} n_{\alpha\gamma} \log(c/\sqrt{n} + C_{\text{eq}} z)$$

To obtain the Cramér-Rao bound, we first compute,

$$\nabla_{zz} L(D, z) = \sum_{\alpha, \gamma} \frac{n_{\alpha\gamma}}{p_{\alpha\gamma}(z)^2} (C_{\text{eq}}^T a_{\alpha\gamma}) (C_{\text{eq}}^T a_{\alpha\gamma})^*$$

Using (6), $\mathbf{E} n_{\alpha\gamma} = \ell_\gamma p_{\alpha\gamma}(\rho^{\text{true}})$, $\rho^{\text{true}} = c/\sqrt{n} + C_{\text{eq}} z^{\text{true}}$, and hence the Fisher information matrix is, with respect to z ,

$$\begin{aligned} F &= \mathbf{E} L(D, z = z^{\text{true}}) \\ &= \sum_{\alpha, \gamma} \frac{\ell_\gamma}{p_{\alpha\gamma}(\rho^{\text{true}})} (C_{\text{eq}}^T a_{\alpha\gamma}) (C_{\text{eq}}^T a_{\alpha\gamma})^* \\ &= G(\ell, \rho^{\text{true}}) \end{aligned}$$

where the last line comes from the definition of $G(\ell, \rho^{\text{true}})$ in (29). Let $\hat{r} = c/\sqrt{n} + C_{\text{eq}} \hat{z}$ be an unbiased estimate of r^{true} . Thus,

$$\text{cov } \hat{r} = C_{\text{eq}} \text{cov } \hat{z} C_{\text{eq}}^T \geq C_{\text{eq}} F^{-1} C_{\text{eq}}^T$$

Using $\text{var } \hat{\rho} = \text{var } \hat{r} = \text{Tr cov } \hat{r}$ and the fact that W is unitary, and hence, $C_{\text{eq}}^T C_{\text{eq}} = I_{n^2-1}$, we get,

$$\text{var } \hat{\rho} \geq \text{Tr } C_{\text{eq}} F^{-1} C_{\text{eq}}^T = \text{Tr } F^{-1}$$

which is the final result (28)-(29).

A.4 Derivation of (80)

Define $x, r_{\alpha\gamma} \in \mathbb{C}^{n^4}$ as,

$$x = \text{vec } X, \quad r_{\alpha\gamma} = \text{vec } R_{\alpha\gamma}$$

The likelihood function in (75) can then be written as,

$$L(D, x) = - \sum_{\alpha, \gamma} n_{\alpha\gamma} \log r_{\alpha\gamma}^* x$$

and the equality constraint in (75) becomes,

$$Ax = \text{vec } I_n, \quad A = [a_1 \cdots a_{n^4}] \in \mathbb{C}^{n^2 \times n^4}$$

with $a_k = \text{vec}(B_i^* B_j) \in \mathbb{C}^{n^2}$ for $k = i + (j-1)n^2$, $i, j = 1, \dots, n^2$. Perform the singular value decomposition $A = U[S \ 0]W^*$, $W = [C \ C_{\text{eq}}]$ with $C \in \mathbb{C}^{n^2 \times n^2}$, $C_{\text{eq}} \in \mathbb{C}^{n^2 \times n^4 - n^2}$ as given in (82). From the definition of the basis functions (69) it follows that $S = \sqrt{n} I_{n^2}$. Observe also that the columns of C_{eq} are a basis for the nullspace of A . Hence all x satisfying the equality constraint are given by,

$$x = \bar{x} + C_{\text{eq}} z, \quad \forall z \text{ with } \bar{x} = (1/\sqrt{n}) C U^* \text{vec } I_n$$

The likelihood function with the equality constraint ($Ax = \text{vec } I_n$) eliminated is then a function only of z ,

$$L = - \sum_{\alpha, \gamma} n_{\alpha\gamma} \log(\bar{x} + C_{\text{eq}} z)$$

This is exactly the same form of the likelihood function in §A.3 after the single equality constraint there is eliminated. Hence, to obtain the Cramér-Rao bound (80) repeat, *mutatis mutandis*, the procedure in §A.3.

References

- [1] B.D.O. Anderson, R.R. Bitmead, Jr. C.R. Johnson, P.V. Kokotovic, R.L. Kosut, I.M.Y. Mareels, L. Praly, and B.D. Riedle. *Stability of Adaptive Systems: Passivity and Averaging Analysis*. MIT Press, 1986.
- [2] K. J. Åström and B. Wittenmark. *Adaptive Control*. Addison-Wesley,, 1995.
- [3] K. Audenaert and B. De Moor. Optimizing completely positive maps using semidefinite programming. *Phys. Rev. A*, 65, 2003.
- [4] K. Banaszek. Reconstruction of photon distribution with positivity constraints. *acta physica slovaca*, 48(3):185–190, June 1998.
- [5] S. Boyd and L. Vandenberghe. *Convex Optimization*. Cambridge University Press, 2004. also available at www.stanford.edu/~boyd/cvxbook.html.
- [6] A. M. Childs, J. Preskill, and J. Renes. Quantum information and precision measurement. *J.Mod.Opt.*, 47:155–176, 2000. e-Print Archive: quant-ph/9904021.
- [7] I.L. Chuang and M.A. Nielsen. Prescription for experimental determination of the dynamics of a quantum black box. *J. Mod. Opt.*, 44:2455–2467, 1997.
- [8] H. Cramér. *Mathematical Methods of Statistics*. Princeton Press, 1946.
- [9] Y. C. Eldar, A. Megretski, and G. C. Verghese. Designing optimal quantum detectors via semidefinite programming. *IEEE Trans. Inform. Theory*, 49:1017–1012, Apr. 2003.
- [10] M. Fazel, H. Hindi, and S. P. Boyd. A rank minimization heuristic with application to minimum order system approximation. *Proc. American Control Conference*, 6:4734–4739, June 2001.
- [11] R. P. Feynman, R. B. Leighton, and M. Sands. *The Feynman Lectures on Physics*. Addison-Wesley, 1963-1965.
- [12] J. M. Geremia and H. Rabitz. Teaching lasers to optimally identify molecular hamiltonians. *Phys. Rev. Lett.*, 89 263902, 2002.
- [13] A. Gilchrist, N. K. Langford, and M. A. Nielsen. Distance measures to compare real and ideal quantum processes. *arXiv quant-ph/0408063*, August 2004.
- [14] G. H. Golub and C. F. Van Loan. *Matrix Computations*. Johns Hopkins University Press, 1983.
- [15] W. P. Grice and I. A. Walmsley. Homodyne detection in a photon counting application. *Journal of Modern Optics*, 1996.
- [16] H. Hjalmarsson, M. Gevers, and F. De Bruyne. For model-based control design, closed loop identification gives better performance. *Automatica*, 32(12):1659–1673, December 1996.

- [17] D. F. V. James, P. G. Kwiat, W. J. Munroe, and A. G. White. Measurement of qubits. *Phys. Rev. A*, 64 052312, 2001.
- [18] Y. Kato, R. C. Myers, D. C. Driscoll, A. C. Gossard, J. Levy, and D. D. Awschalom. Gigahertz electron spin manipulation using voltage controlled g-tensor modulation. *Science*, 299, 2003.
- [19] R. L. Kosut. Iterative adaptive control: Windsurfing with confidence. In G. Goodwin, editor, *Model Identification and Adaptive Control: From Windsurfing to Telecommunications*. Springer-Verlag, 2001.
- [20] R. L. Kosut, H. Rabitz, and I. A. Walmsley. Maximum likelihood identification of quantum systems for control design. *13th IFAC Symposium on System Identification*, 27-29 August 2003. Rotterdam, The Netherlands.
- [21] R. L. Kosut, I. A. Walmsley, Y. Eldar, and H. Rabitz. Quantum state detector : optimal worst-case a posteriori performance. *arXiv:quant-ph/0403150*, March 2004.
- [22] L. Ljung. *System Identification: Theory for the User*. Prentice-Hall, first edition edition, 1987.
- [23] J. Lofberg. Yalmip: a matlab toolbox for rapid prototyping of optimization problems. *Automatic Control Laboratory, ETH Zurich*, 2004. <http://control.ee.ethz.ch/~joloef/yalmip.msql>.
- [24] H. Mabuchi. Dynamical identification of open quantum systems. *Quantum Semiclass. Opt.*, 8(6), December 1996.
- [25] A. Mitra and H. Rabitz. Identifying mechanisms in the control of quantum dynamics through hamiltonian encoding. *Phys. Rev. A*, 67 033407:1–16, 2003.
- [26] Y. Nesterov and A. Nemirovskii. *Interior-Point Polynomial Methods in Convex Programming*. Society for Industrial and Applied Mathematics, 1994.
- [27] M. A. Nielsen and I. L. Chuang. *Quantum Computation and Quantum Information*. Cambridge, 2000.
- [28] A. Papoulis. *Probability, Random Variables, and Stochastic Processes*. McGraw-Hill, 1965.
- [29] M. G. A. Paris, G. M. D’Ariano, and M. F. Sacchi. Maximum likelihood method in quantum estimation. *arXiv: quant-ph/0101071 v1*, 16 Jan 2001.
- [30] M.Q. Phan and H. Rabitz. Learning control of quantum-mechanical systems by laboratory identification of effective input-output maps. *Chem. Phys.*, 217:389–400, 1997.
- [31] M.Q. Phan and H. Rabitz. A self-guided algorithm for learning control of quantum-mechanical systems. *J. Chem. Phys.*, 110:34–41, 1999.

- [32] H. Rabitz, M. Hsieh, and C. Rosenthal. Quantum optimally controlled transition landscapes. *Science*, 303, 2004.
- [33] M. F. Sacchi. Maximum-likelihood reconstruction of completely positive maps. *Phys. Rev. A*, 63 054104, April 2001.
- [34] M. G. Safonov and T. C. Tsao. The unfalsified control concept and learning. *IEEE Trans. Aut. Contr.*, 42(6):843–847, June 1997.
- [35] K. C. Toh, R. H. Tutuncu, and M. J. Todd. Sdpt3: Matlab software for semidefinite-quadratic-linear programming. 2004. <http://www.math.nus.edu.sg/mattohkc/sdpt3.html>.
- [36] L. Vandenberghe, S. Boyd, and S.-P. Wu. Determinant maximization with linear matrix inequality constraints. *SIAM Journal on Matrix Analysis and Applications*, 19(2):499–533, 1998.
- [37] F. Verstraete, A. C. Doherty, and H. Mabuchi. Sensitivity optimization in quantum parameter estimation. *Phys. Rev. A*, 64(032111), 2001. quant-ph/0104116 v1, 24 Apr 2001.
- [38] R. Vrijen, E. Yablonovitch, K. Wang, H. W. Jiang, A. Balandin, V. Roychowdhury, T. Mor, and D. DiVincenzo. Electron-spin-resonance transistors for quantum computing in silicon-germanium heterostructures. *Physical Review A*, 62:1050–2947, 2000.
- [39] I. A. Walmsley and L. Waxer. Emission tomography for quantum state measurement in matter. *Phys. B: At. Mol. Opt. Phys.*, 31:1825–1863, 1998.
- [40] E. Yablonovitch, H. W. Jiang, H. Kosaka, H. D. Robinson, D. S. Rao, and T. Szkopek. Optoelectronic quantum telecommunications based on spins in semiconductors. *Proceedings of the IEEE*, 91(5), May 2003.
- [41] W. Zhu and H. Rabitz. Uniform rapidly convergent algorithm for quantum optimal control of objectives with a positive semi-definite hessian matrix. *Phys. Rev. A*, 58, 1998.